



Published in final edited form as:

*Physiol Rev.* 2010 January ; 90(1): 179–206. doi:10.1152/physrev.00034.2009.

## Lens Gap Junctions in Growth, Differentiation, and Homeostasis

Richard T. Mathias, Thomas W. White, and Xiaohua Gong

Department of Physiology and Biophysics, SUNY at Stony Brook, Stony Brook, New York; and School of Optometry, University of California at Berkeley, Berkeley, California

### Abstract

The cells of most mammalian organs are connected by groups of cell-to-cell channels called gap junctions. Gap junction channels are made from the connexin (Cx) family of proteins. There are at least 20 isoforms of connexins, and most tissues express more than 1 isoform. The lens is no exception, as it expresses three isoforms: Cx43, Cx46, and Cx50. A common role for all gap junctions, regardless of their Cx composition, is to provide a conduit for ion flow between cells, thus creating a syncytial tissue with regard to intracellular voltage and ion concentrations. Given this rather simple role of gap junctions, a persistent question has been: Why are there so many Cx isoforms and why do tissues express more than one isoform? Recent studies of lens Cx knockout (KO) and knock in (KI) lenses have begun to answer these questions. To understand these roles, one must first understand the physiological requirements of the lens. We therefore first review the development and structure of the lens, its numerous transport systems, how these systems are integrated to generate the lens circulation, the roles of the circulation in lens homeostasis, and finally the roles of lens connexins in growth, development, and the lens circulation.

## I. INTRODUCTION

### A. Gap Junctions

Gap junctional communication is required for physiological processes such as cell synchronization, differentiation, growth, and metabolic coordination (143, 217). Gap junctions facilitate these processes by providing a pathway for the intercellular exchange of ions ( $\text{Na}^+$ ,  $\text{K}^+$ ,  $\text{Ca}^{2+}$ ,  $\text{Cl}^-$ ), second messengers [cAMP, cGMP, inositol trisphosphate ( $\text{IP}_3$ )], and small metabolites (glucose, amino acids), allowing both electrical and biochemical coupling between cells (74, 89). Gap junctions are highly specialized clusters of intercellular channels that form where the membranes of two neighboring cells are closely apposed (28), leaving a 2-nm gap, for which gap junctions were originally named (170). In chordates, the connexin family of genes (abbreviated Cx) encodes the vast majority of the gap junction proteins (217, 218). Recently, another group of putative gap junction proteins called pannexins (abbreviated Panx) have been identified and have been shown to be expressed in various vertebrate tissues including the lens (12, 56, 153). Although one pannexin protein (Panx1) has been shown to form gap junction channels in vitro (27), it has been suggested that their major physiological role in vivo may be the formation of nonjunctional membrane

channels associated with ATP and Ca<sup>2+</sup> signaling (43, 93, 159,160, 179,198, 205). To date, only the connexins have been unambiguously identified as bona fide gap junction proteins in the lens, and we will limit our discussion here to connexin-mediated junctional communication.

Connexins have four transmembrane domains forming the channel wall/pore. These domains are connected by two extracellular loops that regulate cell-cell recognition and docking processes and extend the wall/pore across the extracellular gap. Connexin proteins also have cytoplasmic NH<sub>2</sub> and COOH termini and a cytoplasmic loop linking the second and third transmembrane domains (230). The transmembrane domains, NH<sub>2</sub> terminus, and extracellular loops are highly conserved among different connexin proteins, while the sequence and length of both the cytoplasmic loop and COOH terminus are highly variable (213). The cytoplasmic tail and loop are accessible to posttranslational modifications that are believed to play regulatory roles (41). All of the lens connexins are phosphoproteins (99, 148, 203), and phosphorylation is thought to be important for the regulation of assembly and modulation of the physiological properties of the channels (102, 108).

Six connexin proteins oligomerize to form hemichannels (also called connexons) which then are transported to the plasma membrane. Hemichannels from two adjacent cells align with each other in the extracellular space to complete the formation of a cell-to-cell channel (89). Hemichannels can be formed either from a single type of connexin, or from more than one type, leading to the creation of either homomeric or heteromeric hemichannels, respectively (Fig. 1). Additional complexity is possible during the formation of the gap junctional channels. Adjacent cells can contribute different types of hemichannels, forming homotypic (association of two identical homomeric hemichannels), heterotypic (combination of two homomeric hemichannels each of different connexin origin), or heteromeric channels (consisting of 2 distinct heteromeric hemichannels). The formation of these structures depends on the compatibility of connexins forming the channels, and not all connexins can interact with each other. For example, Cx43 was shown to form heterotypic channels with Cx50 but not with Cx46, a process of selective compatibility that is regulated by the sequences of the extracellular loops (214). These complex interactions increase the structural and functional diversity of junctional communication, allowing a vast array of possibilities in the properties of coupling between cells.

## B. Connexins and the Lens

Three connexin isoforms are expressed in distinct spatial and temporal patterns in the mammalian lens (72, 211). Cx43 is expressed at low levels in the lens epithelium (23), but not fibers, while Cx46 is absent from the epithelial cells but becomes highly expressed during fiber cell differentiation (80, 158). In contrast to the segregated expression of Cx43 and Cx46, Cx50 is present in all cells of the lens, first being synthesized in the epithelium and persisting at high levels into the differentiating fibers (44, 172, 212, 215). Each of these three connexins has unique gating and permeation properties (91, 184, 188, 197, 214), suggesting that the developmentally regulated change in the repertoire of connexin subunits is critical for fulfilling the normal physiological role of connexin-mediated communication in the lens.

By using more than one connexin protein to form intercellular channels, the lens can generate functional diversity in the junctional communication between cells. This diversity arises from both the intrinsic differences in functional properties of the three connexins and their ability to selectively form mixed channels containing more than one subunit. In vivo, clear evidence for the ability of Cx46 and Cx50 to coassemble into heteromeric connexons and intercellular channels has been obtained (98, 105), but the percentage of the total number of gap junction channels that are mixtures of these two proteins in the lens is not known. To date, heteromeric channels containing Cx43 with either Cx46 or Cx50 have not been isolated from native lenses by copurification/coimmunoprecipitation studies as has been documented for Cx46 and Cx50 (98, 105).

Distinct gating properties of the lens connexins have also been well documented in vitro. Homotypic channels composed of Cx43, Cx46, or Cx50 were differentially regulated by transjunctional voltage, with Cx43 being the least sensitive and Cx50 exhibiting the greatest sensitivity (59, 190, 214). Regulation by cytoplasmic acidification showed a similar relationship, with  $pK_a$  values of 6.6, 7.0, and 7.3 for Cx43, Cx46, and Cx50, respectively (64, 120, 188). The unitary conductances of single channels were also very different: Cx43 had the smallest at 60–90 pS (63, 146), Cx46 was intermediate at 140 pS (91), and Cx50 had the largest at 220 pS (184) (all measured in CsCl). Heterotypic and heteromeric channels formed from Cx46 and Cx50 displayed a range of unitary conductance that never exceeded the homotypic Cx50 value of 220 pS (91). For all biophysical parameters that have been measured to date, Cx46 channels have had an intermediate value between the intrinsic properties of Cx43 and Cx50.

## II. EARLY LENS DEVELOPMENT

After invagination of the lens placode from the surface ectoderm, the lens first forms as a hollow ball of epithelial cells (Fig. 2, Ref. 65). The posterior epithelial cells then elongate toward the anterior surface, forming the primary fiber cells and producing a cellular sphere. The anterior epithelial cells then proliferate, migrate to the equator, and elongate until they stretch from the anterior to posterior sutures, forming the secondary fibers (138, 140). Fiber cell differentiation is associated with changes in protein synthesis, including the dramatic upregulation of a family of cytoplasmic proteins, the crystallins (51, 161). Cx43 is expressed at the lens placode stage (228). Cx46 and Cx50 are first synthesized at the lens vesicle stage at the time of primary fiber elongation (62, 100, 172). As differentiated fibers transform into the mature fibers found deeper in the core of the lens, they undergo further changes. These include the proteolytic cleavage of the COOH termini of many intrinsic membrane proteins including the connexins (104, 118). COOH-terminal cleavage coincides with gap junctional plaque reorganization, changes in the pH gating of the channels, and the stabilization of transmembrane proteins (84, 96, 134, 235), yet the precise mechanism of how endogenous truncation produces these changes remains illusive (47). In mice, the first lens fiber cells enter the final stages of differentiation on embryonic day 12 (15). The processes of epithelial proliferation and fiber differentiation continue throughout life, although at a progressively slower rate in older animals.

### III. THE MATURE LENS

The mature lens is an avascular, multicellular, transparent organ, whose cells are well coupled by an extensive network of gap junctions. All cells of the lens are living entities that maintain a resting voltage, high internal  $K^+$ , low internal  $Na^+$ , and very low internal  $Ca^{2+}$ . Metabolism is anaerobic and rather low in the central cells, but nonetheless essential. To deliver nutrients and antioxidants to the central cells, the avascular lens has developed its own microcirculatory system (reviewed in Ref. 130). The distribution of membrane transporters reviewed below is primarily dictated by the lens circulation.

It has been useful to think of transport as occurring either at the surface or throughout the volume of the lens. At the surface of the lens, solutes can move into and out of the organ either across membranes of surface located cells, or through the extracellular spaces between surface cells. The volume of the lens comprises intracellular and extracellular compartments, which are linked by transport across the plasma membranes of the fiber cells. While there is a large disparity in the volumes of these two compartments, with the extracellular volume being about 1/100th of the intracellular volume (see Fig. 3B), the extracellular compartment is nevertheless extremely important for homeostasis of the organ: the extracellular spaces carry nutrients and antioxidants into the lens to the fiber cells at its core (130). The intracellular compartment forms a syncytium owing to an extensive network of gap junctions interconnecting the fiber cells.

As shown in Figure 3A, the intracellular compartment of the lens can be separated into three functionally distinct radial domains: the epithelium (E), which caps the anterior hemisphere; the differentiating fibers (DF), which extend from the surface to ~ 15% of the distance into a lens; and the mature fibers (MF), which fill the core. There are differences in membrane transport between domains, and within the E and DF there are variations in transport with location around the lens.

#### A. The Epithelium

The anterior surface of the lens is capped with a single layer of epithelial cells (see Fig. 3A), whose apical membranes face the fiber cells and basolateral membranes contact the aqueous humor. Lens epithelial cells have differences in shape (232) and mitotic activity (reviewed in Ref. 83) from anterior pole to equator. The shape variations are simulated in Figure 3A. Cells at the anterior surface are relatively flat so they present ~3  $cm^2$  of epithelial cell membrane area for every 1  $cm^2$  of lens surface (67). In the mature lens, these cells are in the  $G_0$  phase and do not divide; hence, some of them are as old as the primary fiber cells, which are as old as the organism. About halfway between the anterior pole and equator, the cells are more or less cubic. This is the germinative zone where mitosis occurs in the mature lens. At the equator, the cells are greatly elongated, so they present ~36  $cm^2$  of epithelial cell membrane for every 1  $cm^2$  of lens surface (67). These cells have low mitotic activity and are beginning to express genes characteristic of DF. These elongated epithelial cells are eventually internalized to become new DF.

**1. Epithelial  $Na^+K^+ATPase$ —** $Na^+K^+$  pumps are found in the membranes of almost all mammalian cells, where they have a number of common properties. Each  $Na^+K^+$  pump

uses the energy stored in one ATP to translocate three  $\text{Na}^+$  out of and two  $\text{K}^+$  into a cell, thus generating a net outward current. The  $\text{Na}^+$ - $\text{K}^+$  pump is composed of  $\gamma$ - and  $\beta$ -subunits, and sometimes a  $\gamma$ -subunit called phospholemman (70), with the ATPase activity and ion transport being carried out by the  $\alpha$ -subunit. Three isoforms of the  $\alpha$ -subunit are widely expressed in mammals: the  $\alpha_1$ -,  $\alpha_2$ -, and  $\alpha_3$ -isoforms (189). All three isoforms are specifically inhibited by ouabain, but in most species, the affinity of the  $\alpha_1$ -isoform for ouabain is ~100-fold lower than that of the  $\alpha_2$ - or  $\alpha_3$ -isoform. Functional  $\text{Na}^+$ - $\text{K}^+$  pumps in the lens are expressed primarily in the epithelium, with lens fiber cells being one of the few cell types not to have  $\text{Na}^+$ - $\text{K}^+$ -ATPase activity (reviewed in Ref. 46).

In lenses from different species,  $\text{Na}^+$ - $\text{K}^+$  pump current density has been consistently found to be highest at the equatorial surface of the lens. In the frog lens, cells isolated from the anterior epithelium had a relatively low  $\text{Na}^+$ - $\text{K}^+$  pump current density (67). The low current density in the anterior cell membranes in connection with the flattened cell geometry implied the  $\text{Na}^+$ - $\text{K}^+$  pump current per unit area of lens surface at the anterior pole should be quite low. Indeed, when the ouabain-sensitive ( $\text{Na}^+$ - $\text{K}^+$  pump) current was measured in an Ussing chamber that isolated different surface areas around the rabbit lens,  $\text{Na}^+$ - $\text{K}^+$  pump current was not detectable at the anterior pole (32). In contrast, membranes of isolated equatorial cells from the frog lens had the highest  $\text{Na}^+$ - $\text{K}^+$  pump current density (67), and the  $\text{Na}^+$ - $\text{K}^+$  pump current measured at the equator of the rabbit lens was quite high, being ~10  $\mu\text{A}/\text{cm}^2$  of lens surface (32). Tamiya et al. (191) found the same pattern of  $\text{Na}^+$ - $\text{K}^+$  pump current per area of lens surface around the porcine lens.

While the distribution of  $\text{Na}^+$ - $\text{K}^+$  pump activity appears to be consistent in lenses from different species, the protein composition of these pumps is not (45, 67, 69, 191; reviewed in Ref. 44). The first evidence the lens expresses more than one isoform came from the rabbit lens, where ouabain inhibition of the pump current occurred with two affinities, which differed by ~100-fold (157). Using isoform-specific antibodies, Garner and Horowitz (69) reported bovine equatorial epithelial cells predominantly express the  $\alpha_1$ -isoform, whereas anterior epithelial cells predominantly express the  $\alpha_3$ -isoform. On the basis of RNase protection assays, Gao et al. (67) reported frog lens equatorial epithelial cells express the  $\alpha_1$ -isoform, similar to bovine, but anterior epithelial cells express the  $\alpha_2$ -isoform instead of  $\alpha_3$  as expressed in bovine. In porcine lenses, Tamiya et al. (191) found all epithelial cells express the  $\alpha_1$ -isoform. In rat lens epithelium, Mosely et al. (147) found mRNA for all three isoforms.

Why does the  $\text{Na}^+$ - $\text{K}^+$  pump current density have the same distribution in lenses from different species whereas the isoform composition is species specific? The concentration of  $\text{Na}^+$ - $\text{K}^+$  pump current at the lens equator is critical for the lens circulation, which appears to be ubiquitous. The factors driving the isoform composition of the  $\text{Na}^+$ - $\text{K}^+$  pumps are not as clear. In the heart (reviewed in Ref. 129), different isoforms of the  $\text{Na}^+$ - $\text{K}^+$  pumps have different regulatory pathways, and that may be the case in the lens as well. There are a number of reports on regulation of ion transport in the lens through muscarinic acetylcholine receptors (reviewed in Ref. 54),  $\alpha$ -adrenergic receptors (38), and  $\beta$ -adrenergic receptors (3, 95). However, these reports have not specifically linked the above-mentioned receptors with

the Na<sup>+</sup>-K<sup>+</sup> pumps. Moreover, the source of regulatory inputs to the lens, their coupling to specific transport proteins, and the physiological role of regulation are not known.

**2. Epithelial ion channels**—The ion selectivity of lens epithelial cells is predominately for K<sup>+</sup>, as is the case for almost all cells. There are no reports suggesting anterior to equator variations in the expression of epithelial K<sup>+</sup> channels; however, the anatomical variation from flat cells at the anterior pole to elongated cells at the equator, and the expression of K<sup>+</sup> channels in new equatorial fibers (208), imply the K<sup>+</sup> efflux per unit area of lens surface will be highest at the equator, where K<sup>+</sup> influx via Na<sup>+</sup>-K<sup>+</sup> pumps is also highest. Extensive patch-clamp studies conducted mostly in the laboratory of Dr. James Rae (reviewed in Refs. 130, 131) have identified the molecular basis of lens epithelial K<sup>+</sup> channels from a variety of different species. Any particular species generally expresses more than one type of K<sup>+</sup> channel, and these types vary from species to species, similar to the isoform story for the Na<sup>+</sup>-K<sup>+</sup> pumps. This diversity of K<sup>+</sup>-channel expression may relate to species differences in regulatory pathways (3, 33); however, it may also relate to the size of the lens (130).

The lens epithelium does not express the common epithelial Na<sup>+</sup> channel ENaC, so the small leak of Na<sup>+</sup> into lens epithelial cells is probably through nonselective cation channels or perhaps through Cx50 hemi-channels (57). Although hemi-channels would rarely be open in normal external Ca<sup>2+</sup>, the cation conductance of lens epithelial cell membranes increases dramatically when [Ca<sup>2+</sup>]<sub>o</sub> is dropped to near zero (166), so there may be Cx50 hemi-channels present. If so, they could be the source of a small, nonselective leak conductance in normal [Ca<sup>2+</sup>]<sub>o</sub>. The epithelium also has a small Cl<sup>-</sup> conductance due to expression of the Cl<sup>-</sup> channels ClC-2 and -3 (178) as well as other, as yet unidentified, Cl<sup>-</sup>-channels (209).

**3. Epithelial gap junctions**—All lens epithelial cells are well coupled to each other through gap junctions; however, the coupling of the epithelium to underlying fiber cells varies from anterior pole to equator. We define “coupling conductance” as the measured conductance between cell layers. The lowest coupling conductance occurs at the anterior pole, where only ~ 1 epithelial cell in 10 forms gap junctions with an underlying fiber cell (165). In contrast, at the equator, the coupling conductance is very high, as judged by electrical impedance studies of intact lenses (9). Gap junctions mediating E to DF coupling depend on three types of connexins. The epithelial cells express Cx43 and Cx50. The DF express Cx46 and Cx50 but not Cx43, so E to DF coupling could be through either homotypic Cx50 channels or heterotypic/heteromeric channels. Exogenous expression of various combinations of Cx43, Cx50, and Cx46 has shown that Cx46 will form heterotypic channels with either Cx43 or Cx50, but Cx50 will not form heterotypic channels with Cx43 (214). However, the fact that heterotypic channels form in expression systems does not necessarily mean they do so in the lens, where channel assembly may be regulated in ways not present in expression systems. The protein composition of gap junctions mediating E to DF coupling is therefore an open question.

The pattern of expression and identity of the three isoforms, Cx43, Cx46, and Cx50 (encoded by the Gja1, Gja3, and Gja8 genes, respectively), is the same in all mammalian lenses studied to date. Thus lens connexins lack the species variability in isoform expression seen for Na<sup>+</sup>-K<sup>+</sup> pumps and K<sup>+</sup> channels. Recent studies of lenses from Cx46 and Cx50



KO/KI mice (reviewed later) have begun to specify roles for each isoform in lens development, differentiation, and physiology, and these roles may be consistent between species. Knockout of Cx43 has not provided as much information.

Cx43 is the most widely expressed connexin, and it is found during early development of most tissues. This pattern is seen during development of the lens (100). Knockout of Cx43 is lethal shortly after birth owing to its important roles in the heart (167). Nevertheless, Gao and Spray (68) were able to study lenses of Cx43 KO pups at birth. The lenses developed normally, but when examined carefully, separations between epithelial cells and between epithelial cells and underlying fiber cells were seen, and there were vacuoles in the mass of fiber cells. The separations could imply a role for Cx43 in epithelial fiber communication, but the pups were very sick, literally on the verge of death, so the possibility of indirect effects is a problem. In particular, Cx43-deficient mice do not generate a normal aqueous humor (30), and this would likely affect the lens.

**4. Epithelial water channels**—The passive diffusion of water across cell membranes is facilitated by the aquaporin (AQP) family of integral membrane proteins. A functional water channel is formed by the oligomerization of four AQPs in the endoplasmic reticulum (ER), then the tetramer is inserted into the plasma membrane. In a functional tetramer, each subunit has its own pore that is permeable to water and some neutral solutes, but not to ions. The first such channel (AQP1) was discovered in a red blood cell membrane (164). Of the various aquaporin isoforms, only AQP1 has been identified in the lens epithelium (87, 155, 194, 195). It is expressed in all epithelial cells, but immunostaining at the equator is most intense (195). The intense immunostaining of the equatorial epithelial cell membranes along with the elongated geometry of these cells suggests the water permeability per unit area of lens surface will be highest at the equator, although more direct measurements have not been made.

AQP1 is the most widely expressed aquaporin. It has a relatively high water permeability (34), essentially zero permeability to ions including  $H^+$ , is insensitive to calcium or pH (195), but may be physiologically regulated through phosphorylation (237). Despite the widespread expression of AQP1, its knockout had surprisingly few effects on the physiology of organs in which it is expressed (reviewed in Ref. 202), at least in normal circumstances where the organ was not stressed. The same is true for the lens (173). Knockout of AQP1 reduced epithelial cell membrane water permeability by about threefold, yet no effects were noted in lenses under normal physiological conditions. However, when lenses were stressed with a high glucose environment, all the AQP1<sup>-/-</sup> lenses developed cataracts whereas no wild-type (WT) lenses developed cataracts.

**5. Other epithelial transporters**—The lens epithelium expresses the full complement of membrane transporters found in most cells. Volume regulatory transporters are reviewed in Mathias et al. (130); they include the  $K^+-Cl^-$  cotransporter (36, 109), the  $Na^+-K^+-2Cl^-$  cotransporter (4, 109), and stretch-activated cation channels (40, 166). Glucose uptake by the epithelium is through the facilitated glucose transporter GLUT1 (141). The epithelial  $Na^+-Ca^{2+}$  exchanger and  $Ca^{2+}$ -ATPase are the primary transporters of intracellular calcium for the entire lens (25, 150, 156, 192). The  $Na^+-H^+$  exchanger (5, 14, 219, 221, 229) and

$\text{Cl}^- - \text{HCO}_3^-$  exchanger (14, 219) are the primary regulators of intracellular pH for the entire lens. The  $\text{H}^+$ -ATPase is also probably present, but we could find no references that had studied it.

## B. The Differentiating Fibers

The E to DF transition occurs at the equator of the lens (see Fig. 3A), as the elongated epithelial cells become internalized (232). This signals an abrupt change in expression of membrane and cytoplasmic proteins. All fiber cells are distinguished from epithelial cells by markers such as expression of crystallins, AQP0 (initially identified as the lens major intrinsic protein, MIP) and Cx46, and loss of expression of AQP1 and Cx43. The DF are distinguished from the core MF by the presence of organelles (reviewed in Ref. 16) as well as lack of protein cleavage that occurs at the DF to MF transition.

The newly formed DF are 50–100  $\mu\text{m}$  in length, but they elongate enormously as they are internalized, and when they reach the sutures (reviewed in Ref. 107), where all fiber cells tie together, they have attained a length that is half the circumference of the lens. When apposing fiber cells meet at the suture, elongation ceases. New shells of DF are layered on top of existing shells until a shell is internalized to ~15% of the lens radius, where the DF to MF transition occurs. This progression occurs in lenses from all species, even though the lens radius varies from ~0.1 cm in the mouse to 1.0 cm in the cow. Thus the number of shells of DF, the length of the cells, and the time for elongation will all vary by an order of magnitude between the mouse and cow. The signals for the various steps in this elegant progression are not known, but this complex process is being intensely studied (reviewed in Ref. 122).

The aqueous and vitreous humors are secreted fluids that are maintained in a low oxygen state. Indeed, their partial pressure of  $\text{O}_2$  is generally below 5%, but varies with location and drops to ~1% at the lens surface (183) compared with 20% in the atmosphere. The mitochondria present in DF are an important source of  $\text{O}_2$  buffering for the lens, consuming an estimated ~88% of the  $\text{O}_2$  entering the lens (139). Thus there is a steep  $\text{O}_2$  gradient within the DF. When the bovine lens was bathed in biological saline containing 5%  $\text{O}_2$ , the partial pressure of  $\text{O}_2$  in DF went from 5% at the surface to < 1% at the DF to MF transition (139). This mitochondrial consumption of  $\text{O}_2$  is thought to provide protection against oxidative damage to proteins in the lens core.

**1. Ion channels**—Fiber cell membranes have a very low conductance per unit area, owing to a lack of  $\text{K}^+$  channels (reviewed in Ref. 131). The original studies on fiber cell membrane ion selectivity were rather indirect: Mathias et al. (132) used whole lens impedance studies to estimate the effect of ion substitutions on membrane conductance in the frog lens. They concluded fiber cells had little or no  $\text{K}^+$  permeability, which dominates the membrane conductance of most cells including lens epithelial cells, and that fiber cell membranes were about equally permeable to  $\text{Na}^+$  and  $\text{Cl}^-$ . Patch-clamp studies of isolated membrane patches never found any channels, owing to their scarcity. More direct evidence required a viable isolated fiber cell preparation, which was difficult to obtain (24, 61, 186, 206). The problem was twofold: 1) fiber cells are not self-sustaining and require gap junction coupling with



transporters located in the lens epithelium for homeostasis, and 2) the isolation procedure produced a  $\text{Ca}^{2+}$  leak that caused disintegrative vesiculation of the cells. Recently, Webb and Donaldson (208) developed an isolation procedure that allowed fiber cells to remain stable long enough for whole cell patch-clamp analysis. The critical innovation was to treat the cells with  $\text{Gd}^{3+}$ , a blocker of cation channels that were apparently activated by the isolation procedure and mediated the  $\text{Ca}^{2+}$  leak. They were able to verify fiber cells do indeed lack  $\text{K}^+$  channels, but their loss was not as abrupt as assumed by Mathias et al. (132). The fibers they isolated varied in length from  $\sim 50$  to  $600 \mu\text{m}$ , and their  $\text{K}^+$  conductance dropped to near zero only in cells longer than  $300 \mu\text{m}$ . The DF of young rat lenses vary in length from  $\sim 50$  to  $5,000 \mu\text{m}$ , so the majority lack  $\text{K}^+$  channels. Fibers longer than  $300 \mu\text{m}$  generally had a small  $\text{Cl}^-$  conductance and a nonselective cation conductance, consistent with the early ion substitution results.

**2. Gap junctions**—Gap junction coupling within the DF is via channels formed from Cx46 and Cx50. The coupling conductance is the highest reported for any tissue, but it varies from the equator, where it is maximal, to either pole where it is minimal (9; reviewed in Ref. 130). The average coupling conductance in the radial dimension, measured at  $45^\circ$  from the equator, in mouse or rat lenses, is  $\sim 1 \text{ S/cm}^2$  of cell-to-cell contact (9). At the poles, the conductance could approach zero, which would imply that at the equator it can be as high as  $\sim 2 \text{ S/cm}^2$ , assuming a regular sinusoidal-like variation with an average of  $1 \text{ S/cm}^2$  (130).

The coupling conductance between cells of the DF appears to be regulated. When intracellular pH is decreased, the channels rapidly and reversibly gate closed (134). Although pH regulation is not physiologically relevant, it demonstrates DF channels have the capacity to gate open and closed. Of more physiological relevance, the coupling conductance is significantly increased by fibroblast growth factor (FGF), and FGF is present in the vitreous humor (110). More recently, it has been shown that FGF requires bone morphogenic protein (BMP) signaling to induce an increase in coupling conductance, that expression of BMP receptors is high in the equatorial DF of the lens, and that BMP is released by the lens through an autocrine system (26). These observations led the authors to suggest the relatively high coupling conductance between equatorial DF is regulated by BMP and FGF. Immunostaining of DF lens connexins is relatively uniform around the lens (21, 44, 84), so BMP/FGF upregulation of coupling conductance at the equator is likely through opening existing cell-to-cell channels that are otherwise gated closed.

**3. Water channels**—At the E to DF transition, expression of AQP1 is lost and expression of AQP0 is turned on (reviewed in Ref. 37). Immunostaining shows this to be an abrupt transition (195), but there are probably a few newly differentiated fiber cells that express both aquaporins. AQP0 has a lower water permeability than AQP1 (34); however, it is more highly expressed, constituting  $\sim 50\%$  of total DF membrane protein. Based on comparing WT and AQP0 KO lenses, the water permeability of fiber cell membranes was increased at least fivefold due to the presence of AQP0 (181). AQP0 KO lenses had a severe cataract, with reduced size and widespread disruption of fiber cell structure (2, 181). Indeed, the lenses appeared to have had just an outer shell of fiber cells that are intact. The abrupt

transition from AQP1 to AQP0 and the severe consequences of knocking out AQP0 suggest AQP0 has a unique role in fiber cells, a role that cannot be fulfilled by AQP1 (reviewed in Ref. 130).

**4. Other transporters**—Volume regulatory transporters are reviewed in Mathias et al. (130): they include the  $K^+Cl^-$  cotransporter (36) and the  $Na^+K^+-2Cl^-$  cotransporter (4). Glucose uptake in either the E or DF is through the GLUT family of facilitated glucose transporters. At the E to DF transition, expression of GLUT1 is lost and GLUT3 is synthesized and inserted into the plasma membranes of DF (141, 142). The sodium-dependent glucose transporter SGLT2 is also synthesized in the DF, but it is packaged into the membranes of intracellular vesicles for later insertion into the plasma membranes of MF (130). The amino acids cysteine, glycine, and glutamate are used to synthesize glutathione, which protects the lens against oxidative damage. Transporters of these amino acids by DF are reviewed in Mathias et al. (130). The transporter  $Xc^-$  (114), which exchanges extracellular cystine for intracellular glutamate, is expressed in connection with EAAT4 and EAAT5 (114), which are sodium-dependent glutamate transporters that maintain sufficient internal glutamate to drive cysteine uptake by  $Xc^-$ . The DF also express GLYT1 (116), which mediates sodium-dependent glycine uptake. Amino acid uptake by MF involves several new transporters (described below), and these are expressed in the DF but maintained in a pool of cytoplasmic vesicles for later insertion into the plasma membrane.

### C. The Mature Fibers

The transition from DF to MF is not visible in a microscope, but it marks profound changes in fiber cell properties. These changes include loss of all organelles (17), cleavage of the COOH termini of the fiber cell gap junction proteins Cx46 and Cx50 (96, 103), insertion of Lim2 (MP20) into the plasma membrane (82), degradation of certain membrane transport proteins and insertion of others into the plasma membrane (reviewed in Ref. 130), and probably many other more subtle changes. These changes occur abruptly in just a few cell layers located ~ 15% of the distance into a lens (96).

As described in the section on DF, most of the  $O_2$  entering the lens is consumed by mitochondria; however, the time constant for  $O_2$  consumption is actually about the same in the MF and DF (139), even though the MF lack mitochondria. When mitochondrial respiration was blocked, the DF essentially stopped consuming  $O_2$ , but MF consumption still caused a steep gradient between the surface and center of the lens. The authors tested for activity of several nonmitochondrial  $O_2$  consumers and were able to rule out all those tested except ascorbate, which was almost impossible to deplete significantly in the lens core. They were left with the default speculation that ascorbate, which is known to be present in significant concentrations in the core, was the best candidate for MF  $O_2$  consumption.

**1. Ion channels**—The ion selectivity of the MF appears to be the same as that of the DF: there is little or no  $K^+$  conductance; there is a small  $Na^+$  conductance, which may be due to nonselective cation channels (166), and a small  $Cl^-$  conductance (132). There is no

information on the molecular basis of the channels and no means to isolate the MF, so the data are from impedance studies of intact lenses.

**2. Gap junctions**—Gap junction coupling conductance of the MF appears to be fairly uniform, as apposed to that of the DF which varies dramatically from poles to equator (9, 133). The value of coupling conductance in the MF is  $\sim 0.5 \text{ S/cm}^2$  or about half the average value in the DF. At the DF to MF transition, the COOH terminus of Cx46 and Cx50 is cleaved through activation of calpain, a calcium-dependent protease (118). This is the only known posttranslational modification that might account for the dramatic changes in the properties of coupling.

Gap junctions in the MF lack the regulation present in the DF as they do not gate closed when the cytoplasm is acidified (9, 134, 144, 176). The cytoplasm of central MF is normally acidic (18, 134), which may explain the need to lose pH sensitivity. In the MF, the lack of pH sensitivity of gap junction channels may also be explained by the calpain-mediated cleavage of the COOH termini of Cx46 and Cx50 at the DF to MF transition.

**3. Water channels**—AQP0 is the major fiber cell water channel, and it is expressed in the membranes of all fiber cells including MF. It is not subjected to abrupt cleavage at the DF to MF transition, as was described for the connexins, but its COOH terminus is cleaved in an age-dependent (depth- dependent) manner (10). The cleavage of the COOH terminus, per se, did not reduce its water permeability (11), but cleaved AQP0 formed square array cell-to-cell junctions. In double-layered, two-dimensional crystals of AQP0, the water channels of AQP0 were aligned but were closed (75, 76). However, electron microscopic images of the square array junctions showed the water channels in a staggered configuration, with the AQP0 tetramer in one membrane abutting the particle free apposing membrane, rather than aligned pore to pore (121, 233). In either system the isolated junctions had been subjected to significant biochemical processing before they could be imaged, so the actual structure of the square array junctions is still an open question. Nevertheless, in the MF, AQP0 seems to have two roles: one as a transmembrane water channel and one in cell-to-cell adhesion.

There are some reports of the presence of AQP5 in the fiber cell membranes (155, 207). Knockout of AQP0 reduced fiber cell membrane water permeability from  $\sim 35$  to  $8 \mu\text{m/s}$ , but the lipid matrix of fiber cell membranes had a significantly lower water permeability of  $\sim 1 \mu\text{m/s}$  (196). Thus there was  $\sim 7 \mu\text{m/s}$  of unexplained water permeability, and this could be due to the presence of AQP5.

**4. Other MF transporters**—Glucose uptake by MF is primarily mediated by the  $\text{Na}^+$ -dependent glucose transporter SGLT2 (130), although there is evidence for persistence of some of the DF facilitated glucose transporter GLUT3 in the outer MF (141). Uptake of cystine is mediated by  $\text{Xc}^-$ , as it was in the DF (116). However, the uptake of glutamate by MF is by the  $\text{Na}^+$ -dependent transporter ASCT2 rather than EAAT4/5, which were utilized by DF (116). The  $\text{Na}^+$ -dependent uptake of glycine switches from GLYT1 in the DF to GLYT2 in MF (115). The reasons for the E to DF to MF switch in transporters are mainly unknown. The glucose transporters, however, are expressed in a spatial sequence that follows their known affinity for glucose, with the highest affinity transporter, SGLT2, being

expressed in the core. Since glucose uptake from the extracellular compartment in the E and DF should decrease the extracellular concentration delivered to the MF, the decline in concentration may require a higher affinity transporter (51). This may also be a factor in the E to DF to MF switch in other transporters.

#### IV. THE LENS CIRCULATION

The lens circulation was recently reviewed in detail (130), so a simple overview will be presented here. The lens lacks blood vessels, which would scatter light; hence, it appears to generate its own microcirculatory system, which delivers glucose, amino acids, and antioxidants to the central MF. The circulation is generated by transmembrane transport of solute, which is coupled to fluid flow through osmosis. The overall pattern of flow for both solute and water is illustrated in Figure 4A: the circulation enters the lens at both poles, then exits at the equator. The currents are large by epithelial standards, reaching peak values of  $\sim 30 \mu\text{A}/\text{cm}^2$  of lens surface. This interesting and complex pattern of current flow has been found in all lenses studied, so one assumes it is of fundamental importance.

Evidence for the existence of the circulation includes direct measurement of the circulating ionic current using a vibrating probe to measure the current just outside of rat and frog lenses (154, 171) or an Ussing chamber to isolate sections of the rabbit lens (32) or canine lens (R. T. Mathias, personal observation). Moreover, the spatial distribution of active transport and passive ion channels just reviewed would necessarily generate a circulation. Based on thermodynamic models of solute-solvent coupling, the circulation could not exist if it did not generate significant fluid flow (132). The circulation of fluid has also been directly measured, again using an Ussing chamber to study rabbit and bovine lenses (reviewed in Ref. 31). Lastly, a prediction of the circulation model is the MF must have membrane transporters for the nutrients and antioxidants being delivered through the extracellular spaces. As reviewed in the last section, many of these transporters have been found. There are no known data that are inconsistent with the circulation model. In this section, we will consider the driving force for the circulation, the factors that direct the pattern of flow, and its physiological role.

##### A. Factors Driving the Circulation

The primary engine responsible for maintaining the lens circulation is the epithelial  $\text{Na}^+\text{-K}^+\text{-ATPase}$ . It maintains low  $[\text{Na}^+]_i$ , high  $[\text{K}^+]_i$ , and a negative resting voltage in all lens cells. There is, therefore, a large electrochemical gradient for  $\text{Na}^+$  to enter fiber cells. As illustrated in Figure 4B,  $\text{Na}^+$  is pulled from the extracellular spaces, down its electrochemical gradient across fiber cell membranes, to enter the intracellular compartment. The flux of  $\text{Na}^+$  across the fiber cell membranes pulls  $\text{Na}^+$  into the extracellular spaces from the aqueous and vitreous humors. Hence,  $\text{Na}^+$  enters the lens everywhere through the extracellular spaces between cells. In the extracellular compartment,  $\text{Na}^+$  flows toward the center of the lens. As it moves inward, it is continually moving down its electrochemical gradient across fiber cell membranes to enter the intracellular compartment, where it reverses direction to flow outward toward the surface of the lens. When the intracellular flux of  $\text{Na}^+$  reaches the surface, the  $\text{Na}^+\text{-K}^+\text{-ATPase}$  transports it out of the lens to complete the current loop.

As reviewed in the last section, the lens's  $K^+$  channels and  $Na^+-K^+-ATPase$  are colocalized in the epithelium. Figure 4B shows that this is critical to the circulation. If the fiber cells did not lack  $K^+$  channels,  $K^+$  would circulate in a direction opposite to  $Na^+$ , thus negating the net current and solute fluxes. Instead, the  $K^+$  taken up by the  $Na^+-K^+-ATPase$  mostly exits through channels in the same cells and has very little effect on the surface to center circulation of ions, solute, and water.

Although fiber cells lack  $K^+$  channels, they do have  $Cl^-$  channels (reviewed in sect. III), so there will also be a circulation of  $Cl^-$ .  $Cl^-$  circulates between the extracellular and intracellular spaces within the lens (reviewed in Ref. 130). Because the transmembrane electrochemical gradient for  $Cl^-$  is not large, compared with that for  $Na^+$ ,  $Cl^-$  currents modulate the overall circulation of solute but are not a major driving force.

## B. Factors Directing the Circulation

Figure 4C illustrates our “guess” at the amplitude of the spatial distribution of gap junctional coupling conductance in the DF. Baldo and Mathias (9) demonstrated the poles to equator variation in coupling conductance, but their measurements did not directly indicate the amplitude, hence the “guess.” When the  $Na^+$  enters the intracellular compartment and begins to flow back to the surface of the lens, the relatively high gap junction coupling conductance at the DF equator directs the intracellular flow to the equatorial epithelial cells. Figure 4C also illustrates the spatial distribution of  $Na^+-K^+$  pump current per area of lens surface ( $I_P$ ,  $\mu A/cm^2$ ).  $I_P$  varies from nearly zero at the poles to a maximum of  $10 \mu A/cm^2$  at the equator. Since the  $Na^+-K^+-ATPase$  transports three  $Na^+$  per cycle, the  $Na^+$  current generated at the equator will be  $\sim 30 \mu A/cm^2$ , which is the value of equatorial current measured by the vibrating probe.

The flux of  $Na^+$  is directed by DF gap junction coupling to the equatorial epithelial cells, where the  $Na^+-K^+-ATPase$  is concentrated to transport the flux of  $Na^+$  out of the lens. These two factors appear to be primarily responsible for creating the complex pattern of the circulation. However, the fiber cells around the sutures are less densely packed than elsewhere; hence, the extracellular spaces are more dilated (112), thus enhancing the extracellular entry of the circulation at the poles.

## C. Physiological Role of the Circulation

Our working hypothesis, as shown in Figure 5, is the circulation of  $Na^+$  creates a circulation of solute that is coupled through local osmosis to fluid movement following the same pattern. The circulating pattern of flow creates a well-stirred solution that enters the extracellular spaces of the lens. Just as the circulation of blood to other tissues brings nutrients to the constituent cells, so does the lens microcirculation carry nutrients and antioxidants along the extracellular spaces to the MF, which are too far from the aqueous and vitreous humors for diffusion to be effective (130).

Unless a tissue goes to rather heroic measures to eliminate membrane water permeability, any net transmembrane flux of solute will be coupled through local osmosis to a transmembrane flow of water (135). Net solute flux is given by  $j_{Na} + j_K + j_{Cl}$ . Most epithelia

transport in the open-circuit configuration, so the solute flux is electrically neutral. Any deviation from neutrality will cause charge accumulation and transmembrane voltage changes that restore neutral flux. The lens, however, is unique in that the origins of the internal fluxes, the poles, are short circuited by the aqueous and vitreous humors to the location of exit, the equator. Thus the net flux of solute does not have to be electrically neutral. Every  $\text{Na}^+$  that enters the extracellular spaces at a pole is accompanied by a  $\text{Na}^+$  that exits the lens epithelium at the equator to replace the missing  $\text{Na}^+$  at the pole. Thus there is a continuous chain of sodium ions circulating like horses on a merry go round. At steady state, there is no accumulation of charge, yet the net flux is charged, since at the lens surface  $j_{\text{Na}} + j_{\text{K}} + j_{\text{Cl}} \approx j_{\text{Na}}$ .

In Figure 5, the net membrane flux of solute ( $j_m$ ,  $\text{mol}\cdot\text{cm}^{-2}\cdot\text{s}^{-1}$ ) is mostly  $\text{Na}^+$ . As  $\text{Na}^+$  is pulled from the extracellular spaces by its transmembrane electrochemical potential, it leaves a small deficit of positive charge.  $\text{Cl}^-$  will move to maintain electroneutrality creating a small deficit in negative charge. A similar but opposite phenomenon occurs within the cells, thus creating a small transmembrane osmotic gradient. Based on experimental measurements of lens cell membrane water permeability (195, 196), and model calculations (135), the osmotic gradient will be quite small,  $<1$  mM. Because of this osmotic gradient, water will be pulled across the fiber cell membranes, primarily through the water channel AQP0. Fluid and  $\text{Na}^+$  circulate through the intracellular compartment to the equatorial surface where the  $\text{Na}^+\text{-K}^+$  pumps export the  $\text{Na}^+$ , and through the physical phenomenon just described, create a small transmembrane osmotic gradient. Again through local osmosis, fluid will be pulled across the equatorial epithelial membranes to exit the lens, primarily through the epithelial water channel AQP1. The circulation of ionic current is therefore nearly identical with a circulation of solute, which drives a circulation of fluid.

#### D. Summary

The lens circulation arises because of the physical separation of active extrusion of  $\text{Na}^+$  by epithelial  $\text{Na}^+\text{-K}^+$  pumps from the passive leak of  $\text{Na}^+$  into the lens across fiber cell membranes. The relatively large gap junction coupling conductance in the equatorial region of DF directs the intracellular outward flow to the equatorial epithelium, where  $\text{Na}^+\text{-K}^+$  pumps are concentrated to transport  $\text{Na}^+$  out of the lens. This complex spatial organization of transport proteins generates circulating currents and circulating solute fluxes, which generate an internal microcirculation of fluid. The extracellular fluid moving into the lens carries nutrients and antioxidants to the central MF. Thus the physiological purpose appears to be homeostasis of the MF.

What are the remaining uncertainties? For one, there is an extracellular barrier at the DF to MF transition that stops the entry of dyes (82). Nevertheless, measurements of intracellular voltage and ion gradients (shown in the next sections) fall along smooth curves that suggest no disruption of ion fluxes. Perhaps this barrier allows the passage of small ions but not larger solutes, or perhaps the path of extracellular entry to the MF is at the poles. We do not know the functional properties or purpose of this barrier. There are fiber cell fusions (106) that may provide a parallel path to gap junctions for the movement of solutes. However, when connexins were knocked out, continuity between fiber cells appeared to be lost (78).



We do not know the role of these fusions; however, recent studies have reported a core syncytium for intracellular protein movement, which appears to occur in shells of fibers (180), and this syncytium requires the presence of the lens membrane protein Lim2 (MP20). Cell-to-cell fusions may create this syncytium, but we do not know its role in lens physiology. Finally, we do not know the path of intracellular water flow. Most would assume it follows ion fluxes through gap junctions, but for near-isotonic water flow, ~183 water molecules would have to go through a gap junction channel for every ion. It has not been demonstrated that gap junction channels can conduct that much water flow. The properties needed for gap junction-mediated water transport are outlined in Mathias et al. (136). The fiber cell membranes have sufficient water permeability through AQP0 that water entering the intracellular compartment would find a path to the surface, but is that path through gap junction channels?

## V. ROLES OF CONNEXIN46 AND CONNEXIN50 IN FIBER CELL COUPLING

This section primarily reviews work by us and collaborators using genetically engineered mice that either lacked copies (KO) or expressed different copies (KI) of lens gap junction proteins. The success of these studies has been due to two factors. First, the fiber cell connexins are uniquely expressed in the lens, so KO or KI has no systemic effects that indirectly affect the lens. Nevertheless, altering the expression of a major transport protein, such as a lens connexin, is bound to have effects on the lens that may indirectly affect the process being studied. The results summarized below should not be considered quantitatively exact, but looked at in terms of the general theme of changes that are consistent with working hypotheses. The second factor is that gap junction coupling in intact, freshly dissected lenses can be directly measured using whole lens impedance techniques.

### A. Whole Lens Impedance

Figure 6A illustrates the experimental paradigm. A current passing microelectrode was placed in a central fiber cell to inject stochastic currents, comprising sinusoidal components in the frequency range of interest. A voltage recording microelectrode was placed in a peripheral fiber cell. As shown in Figure 6A, the voltage recording is in the DF at 45° from the posterior pole. In this position, the average DF coupling conductance would be recorded. The voltage electrode can be advanced along its track to the lens center and coupling conductance determined as a function of depth in the lens. The voltage electrode could also be removed and the lens reimpaled at different locations between either pole and equator, thus mapping coupling conductance as a function of position around the lens.

The injected current and induced voltage signals were sent to a Fast Fourier Analyzer, which computes the average impedance in real time. Figure 6B shows typical results when the voltage electrode is advanced along its track towards the lens center. The distance from the lens center ( $r$ , cm) normalized to the lens radius ( $a$ , cm) is listed for each record. The lowest record, at  $r/a = 0.88$ , is from the DF; the other three records are from increasing depths into the MF. There is frequency dependence to the input resistance that has been shown to be due to the membrane conductance and capacitance of all the fiber and surface cells of the lens. This component is not expected to change with depth, and indeed, it does not. The input

resistance asymptotes to a high-frequency series resistance ( $R_S$ ). When the voltage recording is at the location of average DF coupling (presumably close to  $45^\circ$  from the equator),  $R_S$  has been shown to be directly proportional to the resistance of all the gap junctions between the point of voltage recording and the lens surface (133). The transparency of the lens allows us to visualize the locations of current injection and voltage recording, and the nearly spherical geometry allows us to calculate the relationship of  $R_S$  to coupling conductance.

## B. DF Coupling

Figure 7A summarizes results from Gong et al. (78) and Baldo et al. (8) on DF coupling conductance, recorded at  $45^\circ$  from the equator. The lenses were from WT mice, heterozygous KO mice (Cx46<sup>+/-</sup> and Cx50<sup>+/-</sup>), and homozygous KO mice (Cx46<sup>-/-</sup> and Cx50<sup>-/-</sup>). WT mouse lenses had an average DF coupling conductance of  $\sim 1$  S/cm<sup>2</sup> of cell-to-cell contact, which is the highest reported coupling conductance for any tissue studied. KO of half of Cx46 (Cx46<sup>+/-</sup>) resulted in about a 25% reduction in coupling conductance, whereas KO of all of Cx46 (Cx46<sup>-/-</sup>) resulted in about a 50% reduction in coupling conductance, which would be the contribution of Cx50. Similarly, Cx50<sup>+/-</sup> and Cx50<sup>-/-</sup> lenses have reductions in DF coupling conductance of  $\sim 25$  and 50%, respectively. These observations suggest both Cx46 and Cx50 contribute significantly to DF coupling conductance, and their contributions are about equal.

Immunostaining of the inner loop of Cx46 in WT lenses (Fig. 7B, green) indicates the presence of protein in both DF and MF. Immunostaining of the COOH terminus of Cx50 in the same lenses (Fig. 7B, red) shows the presence of protein in the DF, but since the COOH terminus is cleaved at the DF to MF transition, the absence of staining in MF does not necessarily mean absence of protein. Indeed, Kistler and Bullivant (103) identified cleaved products of Cx50 in MF. Overlaying the two images shows yellow staining throughout the DF, indicating the two connexin proteins are in the same plaques, but are the channels homomeric or heteromeric? Jiang and Goodenough (98) showed Cx46/Cx50 heteromeric channels exist, but their methodology did not indicate their relative number. Data shown below on MF coupling and DF channel gating suggest most channels are homomeric.

## C. MF Coupling

Figure 8A summarizes results from Gong et al. (78) and Baldo et al. (8) on MF coupling conductance. In WT lenses, MF coupling conductance is  $\sim 0.5$  S/cm<sup>2</sup> of cell-to-cell contact or half the average coupling conductance of DF. When half of Cx46 was knocked out (Cx46<sup>+/-</sup>), MF coupling conductance fell to  $\sim 0.25$  S/cm<sup>2</sup>, or half the WT value. When all of Cx46 was knocked out (Cx46<sup>-/-</sup>), the MF coupling conductance fell to zero. These results indicated Cx46 was necessary for MF coupling, but it was still possible Cx50 had some role. However, when half of Cx50 was knocked out (Cx50<sup>+/-</sup>), MF coupling conductance did not change even though DF coupling had dropped by 25% (see Fig. 7A). Cx50<sup>-/-</sup> lenses were undersized and in poor condition and had mild central cataracts. Their MF coupling decreased, but that was likely a side effect of other problems; hence, the results are not shown. The Cx50<sup>+/-</sup> lenses were perfectly healthy, so the result of no change in MF coupling conductance was compelling, particularly since the DF coupling conductance was

clearly reduced. The results summarized in Figure 8A suggest Cx46 is responsible for MF coupling. The results shown in Figure 8B strengthen this hypothesis.

Figure 8B summarizes results on KO of Cx46 (78) and KI of Cx46 into the gene locus of Cx50 (210). Knocking out Cx46 provides MF coupling data from lenses expressing Cx46 on zero, one, and two alleles, whereas knocking in Cx46 for Cx50 provides MF coupling data from lenses expressing Cx46 on three and four alleles. Based on quantitative Western blotting, the number of copies of Cx46 was roughly proportional to the number of alleles expressing it. Figure 8B graphs the MF coupling conductance versus the number of alleles expressing Cx46. As can be seen, the relationship is certainly monotonic and within the accuracy of the data, essentially linear. These results support the hypothesis that functional channels in the MF are formed only from Cx46.

As previously described, Cx46 and Cx50 channels have their COOH termini cleaved at the DF to MF transition. DeRosa et al. (47) showed COOH termini cleaved Cx50 channels, when exogenously expressed in oocytes, went to the plasma membrane and formed plaques, but the constituent channels were rarely open. Exogenous expression of COOH termini cleaved Cx46 channels showed no differences in coupling from expression of intact protein (60). Putting all of these results together suggests the following hypothesis: Cx46 and Cx50 form mostly homomeric channels in the plaques coupling the DF, where each contributes about equally to coupling conductance. At the DF to MF transition, the COOH termini of both connexins are cleaved, rendering Cx50 channels nonfunctional, causing the average coupling conductance to drop by about half and leaving Cx46 channels to provide coupling of MF. These results provide an hypothesis on the functional role of Cx46: Cx46 provides long-lived coupling of all fiber cells and maintains a functional circulation to the core MF. However, the results summarized thus far do not address the question: What is the functional role of Cx50?

#### D. Gating of Lens Gap Junction Channels

Figure 9A (204) shows a typical result of superfusing a lens with solution that was bubbled with 100% CO<sub>2</sub> while monitoring DF or MF coupling conductance. The high concentration of CO<sub>2</sub> in the bathing solution and relatively high cell membrane permeability for CO<sub>2</sub> cause rapid diffusion of CO<sub>2</sub> into fiber cells where  $\text{CO}_2 + \text{H}_2\text{O} \rightarrow \text{HCO}_3^- + \text{H}^+$ , thus acidifying the cytoplasm (18, 134). The drop in intracellular pH induces closure of DF gap junction channels, but not MF channels (8, 9, 78, 127, 133, 134). The sensitivity of DF coupling to a drop in pH is illustrated in Figure 9A, top, where the voltage recording microelectrode was placed in a peripheral DF location and the recorded series resistance ( $R_S$  in Fig. 6, Ref. 127) is shown to increase dramatically with time in the CO<sub>2</sub> solution, indicating eventual closure of essentially all DF gap junction channels. In Figure 9A, bottom, the voltage recording microelectrode was placed in a more central MF location, and  $R_S$  shows much less sensitivity to reductions in pH. This can be understood through the equivalent circuit next to the data. In MF, the series resistance, which increases as  $1/r$ , where  $r$  is the distance from the lens center, is dominated by its value in MF. Hence, the closure of DF gap junction channels has a relatively small effect, and increases in  $R_S$  are relatively

small, indicating MF channels are not closing. Prior to our work on Cx50 KO lenses, the results in Figure 9A were observed in every lens studied from every species studied.

Figure 9B compares the effect of pH on DF coupling conductance in WT and Cx50<sup>-/-</sup> lenses (8). The coupling conductance was calculated from  $R_S$  as described in Wang et al. (204), then normalized to the average value in the DF of WT lenses. The CO<sub>2</sub>-containing solution was superfused during the entire period shown, as indicated by the lower gray bar. In WT lenses, the coupling conductance falls from unity to a value of ~0.1, which is the minimum due to parallel pathways. This represents closure of essentially every DF gap junction channel. In the Cx50<sup>-/-</sup> lens, DF coupling conductance begins at ~0.5 owing to the absence of Cx50 channels, but it only decreased slightly due to the superfusion of CO<sub>2</sub>-containing solution, and the final value of ~0.3 is well above that of the WT lens. The implication was that Cx46 channels in the WT lens were closing, whereas the same channels in the Cx50 KO lens were not. This was a striking observation, but one could not rule out that KO of Cx50 had indirect effects on the remaining Cx46 channels, and these effects reduced pH sensitivity. As previously stated, the Cx50 KO lenses were particularly unhealthy, undersized, and had mild central cataracts.

The drug mefloquine (Mfq), a quinine derivative, had been shown to block gap junction channels made from Cx50 but not those made from Cx46 (42). Figure 9C illustrates the effect of Mfq on DF coupling conductance and gating (128). One lens was exposed to Mfq, which needed to be dissolved in DMSO to get it into solution; hence, the contralateral lens was exposed to DMSO as a control. Over a period of ~1 h, Mfq diffused into the extracellular spaces of the DF where it blocked Cx50 channels, causing the coupling conductance of the Mfq-treated lens to drop to about half that of the control lens. Both lenses were healthy, with typical resting voltages and input resistances, and were perfectly transparent. At time zero, each lens was superfused with solution that had been bubbled with 100% CO<sub>2</sub> as indicated by the lower gray bar. The DF coupling conductance of the control lens went to zero as all Cx46 and Cx50 channels closed, whereas the Cx46 channels in the Mfq-treated lens did not close.

Clearly Cx46 and Cx50 interact in the process of gating DF channels. The simplest known mechanism of interaction is for them to form heteromeric channels composed of both proteins. However, as reviewed in the last section, our work on Cx46 and Cx50 KO lenses suggested the hypothesis that most lens channels are homomeric, composed of either Cx46 or Cx50 but not both. If one thinks about the data shown in Figure 9C, they also provide evidence that lens gap junction channels are mostly homomeric. For example, assume all DF channels are heteromeric, made from various combinations of Cx46 and Cx50. To account for the blocking effect of Mfq, it appears that channels with more than half their sub-units being Cx50 are blocked by Mfq, and that is about half the channels. However, in the absence of Mfq, the channels with less than half their subunits being Cx50 are able to close in response to a drop in pH, so in the presence of Mfq, these channels should also be able to close, but they do not. A more reasonable explanation is homomeric channels that gate cooperatively.

This was the first direct demonstration of cooperative gating between neighboring gap junction channels within the same plaques. Cooperativity between neighboring gap junction channels had previously been suggested because dual whole cell patch-clamp studies of junctions containing only two functioning channels often showed simultaneous transitions of both channels from open to closed, or vice versa (125). Probability theory was invoked to demonstrate that this was too improbable to be a random occurrence and must therefore represent cooperative gating of the two channels. Although the logic was sound, the data were not as compelling as those shown in Figure 9C.

Figure 10 provides a cartoon of our ideas on what is happening with regard to coupling in the lens. When Cx46 is synthesized on its normal gene locus in the lens, the channels it forms are pH insensitive, and possibly insensitive to regulatory pathways that regulate coupling through alterations in open channel probability. In the DF of WT lenses, Cx46 and Cx50 channels are somehow linked, probably through a yet unidentified linking protein, such that when Cx50 channels close, they induce closure of neighboring Cx46 channels. In the MF, Cx50 is cleaved and no longer forms active channels; hence, the remaining Cx46 channels are pH insensitive. When Cx50 is knocked out, DF channels made from Cx46 are no longer pH sensitive. When Mfq is used to block DF channels made from Cx50, they are no longer able to respond to pH changes so the Cx46 channels do not close.

### E. Physical Properties of the KO and KI Lenses

Figure 11 shows typical lenses that have had their connexin content genetically altered. The Cx46<sup>+/-</sup> or Cx50<sup>+/-</sup> are indistinguishable from WT lenses; hence, no WT lenses are shown. The Cx50(46/50) heterozygous KI lens is particularly interesting. In this lens, the sequence for Cx46 is knocked in to one of the alleles that normally expresses Cx50. The coupling conductance is higher than that of either Cx46<sup>+/-</sup> or Cx50<sup>+/-</sup> lenses, yet the KI lens gets a central cataract, whereas the KO lenses are clear. Since Cx46 and Cx50 are being synthesized at the same time and in the same place, there is a reasonable probability that heteromeric channels are forming, and these channels may either allow something to move that should not move, or not allow something to move that should move. We do not know why these lenses get cataracts, but it is clear that mixing the connexins is not good for the lens. The Cx46<sup>-/-</sup> lens lacks MF coupling and therefore has no return path for the circulation from MF to the surface; hence, a dense central cataract has formed where homeostasis has been lost. Moreover, that cataract will increase in size with age until it fills the entire MF. We think we understand the development of this particular cataract, and the causes are outlined in section V I. The Cx50<sup>-/-</sup> lenses are undersized and have a mild central cataract. Although the Cx46<sup>-/-</sup> lenses have the more severe cataract, the Cx50<sup>-/-</sup> lenses seemed to be in poorer overall health as they were fragile and ran down quickly. The Cx50(46/46) lens is healthy and perfectly transparent but undersized.

### F. Cx50 in Lens Growth and Development

Cx50 strongly influences lens developmental processes in both epithelial cells and fibers. The deletion of Cx50 in mice resulted in a pronounced growth defect of the lens and eye (216; see Fig. 11) in addition to a delay in fiber maturation, characterized by a retardation of the normal denucleation process that occurs during the transition to mature fibers (172). The

Cx50 knockout animals also developed mild nuclear cataracts (see Fig. 11) that formed in the early postnatal period and did not deteriorate over time (172, 216). Additional defects in lens growth and fiber development have been noted in mice with point mutations in the Cx50 coding sequence (79, 81, 187, 223). In contrast, Cx46 KO showed normal lens growth and fiber differentiation, although they developed postnatal cataracts that progressively worsened as the animals aged (80). These results suggest that Cx46 plays a central role in the maintenance of lens transparency, whereas Cx50 is mainly required for proper lens growth and development.

The growth defect in Cx50 knockout mice produced a 50% reduction in lens mass that resulted from a transient inhibition of the lens growth rate during the first postnatal week (177, 216). The rate of lens growth before and after this critical period was identical to WT mice. Ultrastructural measurements of fiber dimensions confirmed that the reduction of lens size was due to fewer secondary lens fibers forming during this period (55, 216). This acute and transient decrease in lens growth suggested a specific requirement for Cx50 in epithelial cell proliferation and/or fiber differentiation.

### G. Cx50 and Epithelial Mitosis

A major distinction between the Cx46 and the Cx50 KO animals was the reduction in lens growth caused by the absence of Cx50, but not Cx46 (80, 172, 216). The lens growth defect of Cx50-deficient mice was not modulated by genetic background, whereas the cataract severity in both Cx46 and Cx50 knockouts was influenced by genetic modifiers (71, 77). Functional replacement of Cx50 with Cx46 by genetic knock in failed to restore normal lens growth (126, 210). These data identified a common growth defect that was present in all Cx50-deficient lenses. A link between Cx50-mediated junctional communication and epithelial cell mitosis has recently been identified as the major contributor to this reduction in growth (177, 215).

Fewer lens cells were produced in the first postnatal week of Cx50-deficient lenses, and this could have been caused by either an increase in apoptosis or a decrease in mitosis. Apoptosis was examined by TUNEL labeling and immunostaining for cleaved caspase-3 during the first postnatal week and showed no significant differences in the number of apoptotic epithelial cells between WT and Cx50 KO lenses (T.W. White, unpublished data). In contrast, mitosis was dramatically decreased in Cx50-deficient mice when analyzed by bromodeoxyuridine (BrdU) labeling. On postnatal day 3 (P3),  $21 \pm 3\%$  (SD) of the WT epithelial cells were labeled with BrdU after a 1-h exposure. In Cx50 KO lenses, only  $7 \pm 1\%$  of the epithelial cells had incorporated BrdU. When Cx50 was functionally replaced by Cx46, the lenses had  $8 \pm 2\%$  of their epithelial cells labeled by BrdU on P3. This threefold reduction in the labeling index was not caused by a decrease in the rate of cell division and temporally correlated with a 50% reduction in lens volume in Cx50 KO lenses (177). Therefore, Cx50-deficient lenses were smaller because fewer cells were recruited into the cell cycle on P3, when WT lenses underwent a large transient increase in mitosis. These data suggested a positive mitogenic role for gap junctional communication that was Cx50 specific.



The robust effect of Cx50-mediated coupling on epithelial mitosis was surprising in light of the widely held assumption that Cx43 was responsible for the majority of junctional communication between lens epithelial cells (39, 52, 53, 68, 73). This apparent discrepancy was recently resolved by the demonstration that Cx50 is strongly expressed in the lens epithelium and contributes to epithelial coupling in a developmentally regulated manner. Coupling between epithelial cells isolated on P3 was primarily due to Cx50, as evidenced by a 65% reduction in junctional currents elicited by quinine, a drug that blocks Cx50 but not Cx43. As lenses aged, the contribution of Cx50 to total coupling was progressively reduced to 45% on P12 and 25% on P28 (185, 215). Thus Cx50 influenced epithelial cell proliferation as the major participant in junctional communication before being replaced by Cx43 in an age-dependent manner.

Another finding from this study was that the reduction in mitotically active cells in Cx50-deficient lenses was not evenly distributed across the epithelium. Cx46 KI epithelia had a 72% reduction in the number of BrdU-positive cells in the central epithelium and a 13% reduction in labeled cells in the equatorial zone on P3, even though the absolute magnitude of coupling was similar to WT cells (215). These data confirmed an earlier report that Cx46 could not substitute for Cx50 in facilitation of lens cell division (177), in addition to highlighting that the functional activity contributed by Cx50 is particularly important for proliferation in the central epithelium during peak postnatal lens growth.

#### H. How Does Cx50 stimulate proliferation in the central epithelium?

A wealth of data have now accumulated showing that Cx50 coupling stimulates proliferation in the central epithelium of the early postnatal lens (172, 177, 210, 215, 216). Since expression of Cx46 in place of Cx50 did not rescue epithelial proliferation, it is likely that more than simple ionic coupling, which would be provided by either connexin, was required to fulfill Cx50's positive mitogenic role. Lens mitosis is normally stimulated by growth factors that activate intracellular signaling cascades (94, 137, 236). One possibility is that Cx50, but not Cx46, facilitates intercellular propagation of a second messenger that is produced after growth factor stimulation, resulting in recruitment of neighboring cells into mitosis in the central epithelium. Connexins differ in their permeability to second messengers and growth signals (74). An alternative explanation could be that growth factor signaling has a direct gating effect on Cx50 but not Cx46 channels. For example, low concentrations of FGF were shown to induce a threefold increase in coupling in chick lens epithelial cell cultures through stimulation of the ERK pathway (111). Additional studies will be required to distinguish between these possibilities.

#### I. Gap Junction Coupling and Homeostasis of MF

The circulation of  $\text{Na}^+$  illustrated in Figure 3B requires the presence of intracellular voltage and concentration gradients to drive the intracellular flux of  $\text{Na}^+$  from the lens center to surface. The lens center needs to have a higher  $\text{Na}^+$  concentration and a more depolarized voltage relative to the peripheral cells. Figure 12 shows the intracellular voltage recorded from WT and Cx46 KO mouse lenses (78). In the WT lenses, the voltage at the lens center (relative to the external bath) is about  $-60$  mV, which becomes progressively more negative as distance from the center increases, reaching around  $-70$  mV at the surface; thus there is a

10-mV gradient from center to surface associated with the flux of  $\text{Na}^+$ . When Cx46 is knocked out, the voltage in the DF, where coupling is adequate, is not greatly affected, but in the MF, the circulation has been cut off through lack of MF coupling; hence, there is no voltage gradient, and the MF are no longer coupled to the epithelial  $\text{K}^+$  conductance, so they depolarize to a new steady state that is determined by their  $\text{Na}^+$  and  $\text{Cl}^-$  permeabilities.

Although  $\text{Na}^+$  transport drives the circulation, any other cation in the aqueous and vitreous humors may follow the same pattern, provided it can cross fiber cell membranes. There is a very large transmembrane electrochemical gradient for  $\text{Ca}^{2+}$ , so any small transmembrane leak will cause  $\text{Ca}^{2+}$  to circulate in a manner similar to  $\text{Na}^+$ . Figure 13, *left*, illustrates the expected circulation of  $\text{Ca}^{2+}$ .  $\text{Ca}^{2+}$  moves down its transmembrane electrochemical gradient to leave the extracellular spaces and enter the fiber cells, where it must flow from cell to cell through fiber cell gap junctions to reach the epithelial  $\text{Ca}^{2+}$ -ATPase and  $\text{Na}^+$ - $\text{Ca}^{2+}$  exchanger. In this unique system,  $\text{Ca}^{2+}$  homeostasis depends on gap junction coupling. As shown in Figure 13, *right*, in WT lenses, MF coupling conductance is  $\sim 0.5 \text{ S/cm}^2$  of cell-to-cell contact. In Cx50(46/46) KI lenses, it is approximately doubled at  $1 \text{ S/cm}^2$ . Thus, in either type lens, there should be circulation of  $\text{Ca}^{2+}$  with a center to surface concentration gradient driving the  $\text{Ca}^{2+}$  flux to its exit place, the surface cells. Since the coupling conductance of the KI lenses is about twice that of WT lenses, the gradient should be about half that in WT lenses. In the Cx46 KO lenses, MF coupling has been lost, so the egress pathway for  $\text{Ca}^{2+}$  is absent.  $\text{Ca}^{2+}$  can therefore enter the MF, but since it cannot get out, it will slowly accumulate and  $\text{Ca}^{2+}$  homeostasis is lost.

Gao et al. (66) measured the  $\text{Ca}^{2+}$  concentration in freshly dissected intact lenses ( $\sim 2$  mo of age) by injecting a  $\text{Ca}^{2+}$  indicator dye, fura 2, into fiber cells. Figure 14 summarizes their findings. In WT lenses, there was a center to surface  $\text{Ca}^{2+}$  gradient of  $\sim 400 \text{ nM}$ , as the concentration in the center was  $700 \text{ nM}$  and at the surface  $300 \text{ nM}$ . In the Cx46 KI lenses, which have twice the coupling conductance, the concentration gradient was halved to a value of  $\sim 200 \text{ nM}$ , as the concentration in the center was  $500 \text{ nM}$  and at the surface  $300 \text{ nM}$ . In the Cx46 KO lenses, which have lost all MF coupling,  $\text{Ca}^{2+}$  had accumulated to over  $1 \mu\text{M}$  and would continue to accumulate with age, as  $\text{Ca}^{2+}$  homeostasis has been lost.

The Cx46 KO lenses have a dense central cataract (see Fig. 11) that is in many ways similar to the age-onset central cataract seen in humans. We know what caused the Cx46 KO cataract: loss of Cx46. We also believe we know the steps leading to formation of the cataract. KO of Cx46 causes loss of coupling of MF (78), thus eliminating the  $\text{Ca}^{2+}$  egress pathway and causing accumulation of  $\text{Ca}^{2+}$  in the MF (66). Baruch et al. (13) and Tang et al. (193) have shown the accumulation of  $\text{Ca}^{2+}$  in the Cx46 KO lenses activates calpain, a calcium-dependent protease, which cleaves the crystallins. The cleaved crystallins aggregate and come out of solution generating the central opacity. Does this special case have any general relevance to human age-onset cataract formation? We cannot be sure, but connexins are being increasingly implicated in cataractogenesis.

There is a long-standing hypothesis that cataract formation is associated with cumulative oxidative damage to the crystalline proteins. The lens has a number of antioxidant enzymes: superoxide dismutase, catalase, glutathione reductase, and glutathione peroxidase-1

(GPX-1). GPX-1 is a cytoplasmic enzyme that protects the lens against H<sub>2</sub>O<sub>2</sub>-mediated damage. Ho et al. (90) produced a GPX-1 KO mouse. Reddy et al. (169) characterized cataract formation in lenses from the GPX-1 KO mouse and found age-onset central opacities formed in essentially all lenses by 15 mo of age, whereas at 2 mo of age, no lenses had cataracts. Wang et al. (204) used whole lens impedance and other techniques to determine if there were any differences in the transport properties of 2-mo-old GPX-1 KO lenses from those of WT lenses, differences that preceded cataract formation and could therefore be causal.

Size, transparency, resting voltage, membrane resistance, and membrane water permeability for the GPX-1 KO lenses were the same as age-matched WT lenses. However, gap junction coupling conductance in the KO lenses was about half that of WT lenses. Western blots showed ~50% reductions in both Cx46 and Cx50, whereas there was no reduction in the water transport protein, AQP0, consistent with the transport data. Wang et al. (204) concluded lens connexins were primary targets of oxidative damage, they were specific targets since AQP0 was not affected, and the reductions in coupling would likely compromise the lens circulation and Ca<sup>2+</sup> homeostasis. To test the effects on the lens circulation, they measured intracellular Na<sup>+</sup> by injecting a Na<sup>+</sup> indicator dye, SBFI. To test the effects on Ca<sup>2+</sup> homeostasis, fura 2 was injected into fiber cells. The results are shown in Figure 15.

Figure 15 shows the reductions in coupling conductance were accompanied by increases in the center to surface gradients in both Na<sup>+</sup> and Ca<sup>2+</sup> concentrations. The smooth curves represent structurally based model calculations on the expected concentrations given a functional circulation. The fit of the model to the data suggests the circulation is still functional in the KO lenses, but at the expense of some loss of Na<sup>+</sup> and Ca<sup>2+</sup> homeostasis. MF membrane transporters for amino acids and glucose generally use the transmembrane Na<sup>+</sup> gradient to drive uptake; hence, the increased intracellular Na<sup>+</sup> concentration in the MF would have reduced the effectiveness of these transporters. Moreover, the accumulation of Ca<sup>2+</sup> in the MF should have caused increased calpain activity. The lens has systems designed to protect itself against the effects of oxidative damage, such as chaperone activity of the  $\alpha$ -crystallins (92), which safely package damaged proteins and keep them from coming out of solution. However, these systems have limits, and if they are taxed early in the life of the lens, they are unlikely to be able to provide protection late in life. Thus loss of gap junction coupling in these young lenses is indeed a good candidate for the cause of the eventual cataracts that form in old GPX-1 KO lenses.

The mechanism by which oxidative stress reduces the number of connexins and coupling conductance in the lens is not known. Since AQP0 was not affected, it does not seem to be nonspecific damage to membrane proteins; instead, it appears to be a specific effect on the lens connexins. Lin and Takemoto (117) have shown that protein kinase C (PKC)- $\gamma$  is activated by oxidative stress, PKC- $\gamma$  phosphorylates lens gap junctions, and phosphorylation causes the gap junction plaques to break up and degradation of the connexins (234). This connexin-specific path for oxidative stress is an attractive possibility, but it has not been investigated. Whatever the path, a reduction in major transport proteins, such as the connexins, is a plausible cause for age-onset central cataracts. These cataracts represent a

loss of homeostasis of the MF. Homeostasis of MF depends on the lens circulation, which depends on gap junction coupling, so it is reasonable to think that compromise of membrane transport would cause loss of intracellular homeostasis.

## J. Summary

The KO and KI mouse lenses have provided a wealth of new information and hypotheses on the roles of the lens fiber cell connexins. These hypotheses include the following: Cx46 and Cx50 form homomeric channels that cooperatively interact to implement gating of DF channels. Cx46 is primarily responsible for providing coupling of fiber cells from the lens center to surface; thus it is an essential component of the lens circulation and required for homeostasis of the MF. Cx50 has subtler roles in growth, development, and regulation of coupling conductance. The connexins are early targets of oxidative stress and may be the causal factor in development of age-onset central cataracts.

Nevertheless, key questions remain. 1) With the assumption of cooperative gating of homomeric Cx46 and Cx50 channels, there must be a linker protein that has not been identified. One candidate is zonula occludans-1 (ZO-1), a PDZ-domain containing tight junction protein that is known to be present in lens gap junction plaques (149). If an unidentified linker protein modulates gating, it might have other unidentified roles in lens gap junction coupling, and once these roles are known, our simple hypotheses may fall. 2) The regulatory pathways responsible for creating the equator to poles variation in DF coupling conductance are just beginning to be unraveled. Cx50 is clearly necessary for pH-mediated gating of DF gap junction channels. Could Cx50 also be necessary for the equator to poles variation in DF coupling conductance? 3) When Cx46 has been exogenously expressed (60), the channels have had pH sensitivity, whereas in the WT lens they do not. However, when Cx46 was endogenously expressed on the Cx50 gene locus, the channel had pH sensitivity. What posttranslational modifications are made by the lens to eliminate pH sensitivity of Cx46 channels that are normally expressed in the WT lens? 4) Cx50 appears to modulate cell division by transferring some signal from an epithelial cell that has entered the cell cycle to neighboring epithelial cells, inducing them to also enter the cell cycle. What is that signal? 5) What is the cause of the cataract in the Cx50(46/50) lenses.

So far, this review has focused on the properties of normal lenses and the effects on these properties of knocking out or knocking in lens Cx proteins. These data have been used to generate hypotheses on the roles of lens gap junction proteins in lens growth, differentiation, and homeostasis. The next section describes the rich variety of cataract phenotypes that occur due to congenital mutations of lens fiber cell connexins. The plethora of mutation-induced phenotypes far exceeds those found in the Cx KO and KI models. There must be some common threads connecting the defects in these lenses, and connecting them with the defects found in Cx KO or KI lenses, but they are not yet well understood.

## VI. CONNEXIN MUTATIONS AND CATARACTS

Connexin gene mutations are one of the common causes for hereditary cataracts in humans and mice. Dozens of mutations of Cx46 and Cx50 genes have been reported to cause hereditary cataracts in human (Table 1). The majority of these are point mutations, which

can be linked to variable expression of the type and severity of dominant cataracts. Some identical mutations lead to variable phenotypes in different races. Some of the mutations dramatically reduce the eye size. Two point COOH-terminal frame shift mutants of Cx50 lead to recessive cataracts.

Availability of mainly late-stage cataracts in humans hinders the investigation of molecular mechanisms in cataract formation. Fortunately, many mutations of Cx46 or Cx50 genes have also been discovered or created in rodent cataract models (Table 2). Some of these mutations coincidentally result in a replacement of an identical residue or an adjacent residue of connexin proteins between human and mouse. By using these animal models, researchers have investigated why and how mutated Cx46 and Cx50 genes lead to various types of cataracts. Recent findings demonstrate that mutated connexin subunits change the conductance and/or gating of gap junction channels, alter protein trafficking or channel assembly, or trigger intracellular stress responses *in vivo* or *in vitro*. Thus genetic evidence, cellular information, and physiological data indicate that connexin mutations affect different molecular mechanisms to impair lens development and transparency.

### A. Connexin Mutations Disrupt Lens Development

As previously reviewed, Cx50 is essential for the lens size (172, 210). Cx50 KO mice developed smaller lenses, ~60% the size of WT lenses. Moreover, a loss of Cx50 delays lens fiber cell maturation (172) and reduces the proliferation of epithelial cells (177). Recent studies demonstrated that Cx50 is not only important for the formation of the primary fiber cells but also can interact with Cx46 to regulate the formation of the secondary fiber cells (222). Genetic data on the Cx50-S50P point mutation (in extracellular loop 1) suggest that diverse gap junction channels probably mediate distinct mechanisms to control the formation of lens primary and secondary fiber cells. Cx50-S50P mutant subunits require the presence of wild-type Cx50 subunits to specifically inhibit the elongation of the primary fibers in the embryonic lens, but this combination does not affect the elongation of secondary fiber cells. In contrast, the Cx50-S50P mutant subunits need wild-type Cx46 subunits to disrupt the differentiation and elongation of the lens secondary fibers, but this combination does not affect the lens primary fiber cells. Moreover, without wild-type Cx46 and Cx50 connexin subunits, the Cx50-S50P mutant subunit itself seems a loss-of function mutation in the lens. Thus diverse gap junction channels probably mediate distinct mechanisms to control the formation of lens primary and secondary fiber cells during development.

### B. Connexin Mutations Impair Lens Transparency

As previously described, the nuclear cataract caused by a loss of Cx46 is related to an elevation of intracellular calcium concentration and the subsequent increase of calcium-dependent protein degradation in lens fiber cells (13, 66, 80). Calpain II, a calcium-activated protease, mediates at least in part the formation of the nuclear cataract in the Cx46<sup>-/-</sup> lenses by cleaving crystallin proteins (193). However, the severity of the cataract is much greater in the J129 strain of mice than the C57BL6 strain. No mutation was identified in calpain II genes between mouse J129 and C57BL6 strains, so calpain II is unlikely to be a genetic modifier that influences the severity of this nuclear cataract (77). The role of calpain II in the

lens is intriguing and remains to be elucidated. Hopefully, identification of genetic modifier(s) influencing nuclear cataracts in the Cx46<sup>-/-</sup> lenses in the future will reveal novel molecular insights.

Thus far, only null or COOH-terminal frame-shift mutants of Cx46 and Cx50 have been found to cause recessive cataracts. All point mutations of Cx50 and Cx46 are linked to dominant cataracts with variable severity. Mouse Cx50 point mutations including G22R, D47A, and S50P cause a posterior ruptured lens, a nuclear cataract, or a whole cataract with smaller lenses (35, 215, 224). Different combinations of mutant and WT connexin gene alleles (either Cx46 or Cx50) have been demonstrated to be related to the formation of different types of cataracts (79). In addition, other genetic factors influence cataractogenesis due to connexin point mutations (174). Thus variable expression of cataract formation is probably from a combination of both altered gap junction communication due to the mixture of mutant and wild-type sub-units and genetic modifiers in the lens.

### C. Mutated Connexins Alter Electrical Properties of Gap Junction Channels

Substantial progress has been made on how mutant connexin subunits affect the properties of gap junction channels. Electrophysiological studies demonstrate that different point mutations affect the channel properties in different ways. Mouse Cx50-D47A mutant protein sub-units, which cause dominant cataracts in No2 mice, were unable to form functional channels and did not inhibit WT Cx46 or Cx50 junctional conductance in paired *Xenopus* oocytes (225). A similar human point mutation Cx50-D47N, which caused dominant nuclear pulverulent cataracts, also failed to form functional channels in paired oocytes (6), and coexpression of Cx50D47N with WT Cx50 did not inhibit gap junctional conductance. Cx50-D47A and D47N mutants as well as Cx46-N63S and fs380 mutants were loss-of-function mutants (152). However, the recessive phenotypes of Cx46 or Cx50 KO mice suggest that functional loss of one allele of either Cx46 or Cx50 gene is not sufficient to cause a dominant cataract. It is possible that substantial intracellular retention of these mutated connexin proteins disturbs trafficking of membrane proteins or activates a pathway of protein degradation in lens fiber cells to lead to dominant cataracts. Cx46-N63S mutant also altered the properties of hemichannels in vitro (58). A functional role of hemichannels in the lens remains to be confirmed.

Studies of mouse Cx50-G22R and S50P mutants showed that these point mutant subunits could form functional channels with WT Cx50 or Cx46, but altered the voltage gating and/or channel conductance in the paired *Xenopus* oocyte system or in transfected HeLa cells (48, 223). Human Cx50-P88S mutant subunits failed to form functional gap junction channels; however, they acted as a dominant negative inhibitor to human WT Cx50 gap junction channels (151). Taken together, these mixed channels formed by the homomeric and/or heteromeric combination of wild-type and mutant Cx50 or Cx46 proteins displayed significantly altered gating properties and channel conductance, which may contribute to the variable expression of cataracts in the lens.



## D. Mutated Connexins Affect Trafficking and Trigger Stress Responses

Some of the mutations may result in misfolded proteins in the cell. These misfolded proteins probably accumulate in the ER or Golgi apparatus to induce stress responses. The Cx46fs380 mutant protein, which contains 87 aberrant amino acids in its COOH terminus and is 31 amino acids longer than WT Cx46, showed extensive colocalization with markers for ER and Golgi (145). However, expression of hCx50P88S resulted in cytosolic aggregates, which differed from aggresomes, in cultured cells (22). Ubiquitin-proteasome system is suggested to be involved in degradation of other connexin mutant proteins in non-lens cells (101). Future studies will be needed to elucidate these stress signals in responding to misfolded proteins in the lens.

## ACKNOWLEDGMENTS

### GRANTS

This work was supported by National Eye Institute Grants EY-06391, EY-13849, and EY-13163.

## REFERENCES

1. Addison PK, Berry V, Holden KR, Espinal D, Rivera B, Su H, Srivastava AK, Bhattacharya SS. A novel mutation in the connexin 46 gene (GJA3) causes autosomal dominant zonular pulverulent cataract in a Hispanic family. *Mol Vis.* 2006; 12:791–795. [PubMed: 16885921]
2. Al-Ghoul KJ, Kirk T, Kuszak AJ, Zoltoski RK, Shiels A, Kuszak JR. Lens structure in MIP-deficient mice. *Anat Rec A Discov Mol Cell Evol Biol.* 2003; 273:714–730. [PubMed: 12845708]
3. Alvarez LJ, Candia OA, Polikoff LA. Beta-adrenergic stimulation of Na(+)-K(+)-2Cl(-) cotransport activity in the rabbit lens. *Exp Eye Res.* 2003; 76:61–70. [PubMed: 12589776]
4. Alvarez LJ, Candia OA, Turner HC, Polikoff LA. Localization of a Na(+)-K(+)-2Cl(-) cotransporter in the rabbit lens. *Exp Eye Res.* 2001; 73:669–680. [PubMed: 11747367]
5. Alvarez LJ, Candia OA, Wolosin JM. Evidence for parallel Na(+)-H(+) and Na(+)-dependent Cl(-)-HCO<sub>3</sub>(-) exchangers in cultured bovine lens cells. *Exp Eye Res.* 1992; 55:747–755. [PubMed: 1335884]
6. Arora A, Minogue PJ, Liu X, Addison PK, Russel-Eggitt I, Webster AR, Hunt DM, Ebihara L, Beyer EC, Berthoud VM, Moore AT. A novel connexin50 mutation associated with congenital nuclear pulverulent cataracts. *J Med Genet.* 2008; 45:155–160. [PubMed: 18006672]
7. Arora A, Minogue PJ, Liu X, Reddy MA, Ainsworth JR, Bhattacharya SS, Webster AR, Hunt DM, Ebihara L, Moore AT, Beyer EC, Berthoud VM. A novel GJA8 mutation is associated with autosomal dominant lamellar pulverulent cataract: further evidence for gap junction dysfunction in human cataract. *J Med Genet.* 2006; 43:e2. [PubMed: 16397066]
8. Baldo GJ, Gong X, Martinez-Wittinghan FJ, Kumar NM, Gilula NB, Mathias RT. Gap junctional coupling in lenses from alpha(8) connexin knockout mice. *J Gen Physiol.* 2001; 118:447–456. [PubMed: 11696604]
9. Baldo GJ, Mathias RT. Spatial variations in membrane properties in the intact rat lens. *Biophys J.* 1992; 63:518–529. [PubMed: 1420894]
10. Ball LE, Garland DL, Crouch RK, Schey KL. Post-translational modifications of aquaporin 0 (AQP0) in the normal human lens: spatial and temporal occurrence. *Biochemistry.* 2004; 43:9856–9865. [PubMed: 15274640]
11. Ball LE, Little M, Nowak MW, Garland DL, Crouch RK, Schey KL. Water permeability of C-terminally truncated aquaporin 0 (AQP0 1–243) observed in the aging human lens. *Invest Ophthalmol Vis Sci.* 2003; 44:4820–4828. [PubMed: 14578404]
12. Barbe MT, Monyer H, Bruzzone R. Cell-cell communication beyond connexins: the pannexin channels. *Physiology.* 2006; 21:103–114. [PubMed: 16565476]

13. Baruch A, Greenbaum D, Levy ET, Nielsen PA, Gilula NB, Kumar NM, Bogyo M. Defining a link between gap junction communication, proteolysis, and cataract formation. *J Biol Chem.* 2001; 276:28999–29006. [PubMed: 11395508]
14. Bassnett S. Intracellular pH regulation in the embryonic chicken lens epithelium. *J Physiol.* 1990; 431:445–464. [PubMed: 1966051]
15. Bassnett S. Lens organelle degradation. *Exp Eye Res.* 2002; 74:1–6. [PubMed: 11878813]
16. Bassnett S. On the mechanism of organelle degradation in the vertebrate lens. *Exp Eye Res.* 2009; 88:133–139. [PubMed: 18840431]
17. Bassnett S, Beebe DC. Coincident loss of mitochondria and nuclei during lens fiber cell differentiation. *Dev Dyn.* 1992; 194:85–93. [PubMed: 1421526]
18. Bassnett S, Duncan G. Direct measurement of pH in the rat lens by ion-sensitive microelectrodes. *Exp Eye Res.* 1985; 40:585–590. [PubMed: 4007073]
19. Bennett TM, Mackay DS, Knopf HL, Shiels A. A novel missense mutation in the gene for gap-junction protein alpha3 (GJA3) associated with autosomal dominant “nuclear punctate” cataracts linked to chromosome 13q. *Mol Vis.* 2004; 10:376–382. [PubMed: 15208569]
20. Berry V, Mackay D, Khaliq S, Francis PJ, Hameed A, Anwar K, Mehdi SQ, Newbold RJ, Ionides A, Shiels A, Moore T, Bhattacharya SS. Connexin 50 mutation in a family with congenital “zonular nuclear” pulverulent cataract of Pakistani origin. *Hum Genet.* 1999; 105:168–170. [PubMed: 10480374]
21. Berthoud VM, Cook AJ, Beyer EC. Characterization of the gap junction protein connexin56 in the chicken lens by immunofluorescence and immunoblotting. *Invest Ophthalmol Vis Sci.* 1994; 35:4109–4117. [PubMed: 7960593]
22. Berthoud VM, Minogue PJ, Guo J, Williamson EK, Xu X, Ebihara L, Beyer EC. Loss of function and impaired degradation of a cataract-associated mutant connexin50. *Eur J Cell Biol.* 2003; 82:209–221. [PubMed: 12800976]
23. Beyer EC, Kistler J, Paul DL, Goodenough DA. Antisera directed against connexin43 peptides react with a 43-kD protein localized to gap junctions in myocardium and other tissues. *J Cell Biol.* 1989; 108:595–605. [PubMed: 2537319]
24. Bhatnagar A, Ansari NH, Wang L, Khanna P, Wang C, Srivastava SK. Calcium-mediated disintegrative globulization of isolated ocular lens fibers mimics cataractogenesis. *Exp Eye Res.* 1995; 61:303–310. [PubMed: 7556494]
25. Borchman D, Delamere NA, Paterson CA. Ca-ATPase activity in the rabbit and bovine lens. *Invest Ophthalmol Vis Sci.* 1988; 29:982–987. [PubMed: 2836334]
26. Boswell BA, Le AC, Musil LS. Upregulation and maintenance of gap junctional communication in lens cells. *Exp Eye Res.* 2009; 88:919–927. [PubMed: 19103198]
27. Bruzzone R, Hormuzdi SG, Barbe MT, Herb A, Monyer H. Pannexins, a family of gap junction proteins expressed in brain. *Proc Natl Acad Sci USA.* 2003; 100:13644–13649. [PubMed: 14597722]
28. Bruzzone R, White TW, Paul DL. Connections with connexins: the molecular basis of direct intercellular signaling. *Eur J Biochem.* 1996; 238:1–27. [PubMed: 8665925]
29. Burdon KP, Wirth MG, Mackey DA, Russell-Eggitt IM, Craig JE, Elder JE, Dickinson JL, Sale MM. A novel mutation in the Connexin 46 gene causes autosomal dominant congenital cataract with incomplete penetrance. *J Med Genet.* 2004; 41:e106. [PubMed: 15286166]
30. Calera MR, Topley HL, Liao Y, Duling BR, Paul DL, Good-enough DA. Connexin43 is required for production of the aqueous humor in the murine eye. *J Cell Sci.* 2006; 119:4510–4519. [PubMed: 17046998]
31. Candia OA, Alvarez LJ. Water and ion transport in ocular tissues. *Physiol Mini-Rev.* 2006; 1:48–57.
32. Candia OA, Zamudio AC. Regional distribution of the Na<sup>+</sup> and K<sup>+</sup> currents around the crystalline lens of rabbit. *Am J Physiol Cell Physiol.* 2002; 282:C252–C262. [PubMed: 11788336]
33. Candia OA, Zamudio AC, Polikoff LA, Alvarez LJ. Distribution of acetylcholine-sensitive currents around the rabbit crystalline lens. *Exp Eye Res.* 2002; 74:769–776. [PubMed: 12126950]
34. Chandy G, Zampighi GA, Kreman M, Hall JE. Comparison of the water transporting properties of MIP and AQP1. *J Membr Biol.* 1997; 159:29–39. [PubMed: 9309208]

35. Chang B, Wang X, Hawes NL, Ojakian R, Davisson MT, Lo WK, Gong X. A Gja8 (Cx50) point mutation causes an alteration of alpha 3 connexin (Cx46) in semi-dominant cataracts of Lop10 mice. *Hum Mol Genet.* 2002; 11:507–513. [PubMed: 11875045]
36. Chee KS, Kistler J, Donaldson PJ. Roles for KCC transporters in the maintenance of lens transparency. *Invest Ophthalmol Vis Sci.* 2006; 47:673–682. [PubMed: 16431967]
37. Chepelinski AB. Structural function of MIP/aquaporin 0 in the eye lens: genetic defects lead to congenital inherited cataracts. *Handb Exp Pharmacol.* 2009; 190:265–297. [PubMed: 19096783]
38. Churchill GC, Louis CF. Stimulation of P<sub>2U</sub> purinergic or alpha<sub>1A</sub> adrenergic receptors mobilizes Ca<sup>2+</sup> in lens cells. *Invest Ophthalmol Vis Sci.* 1997; 38:855–865. [PubMed: 9112981]
39. Cooper K, Rae JL, Gates P. Membrane and junctional properties of dissociated frog lens epithelial cells. *J Membr Biol.* 1989; 111:215–227. [PubMed: 2600960]
40. Cooper KE, Tang JM, Rae JL, Eisenberg RS. A cation channel in frog lens epithelia responsive to pressure and calcium. *J Membr Biol.* 1986; 93:259–269. [PubMed: 2434653]
41. Cruciani V, Mikalsen SO. Connexins and gap junctional intercellular communication and kinases. *Biol Cell.* 2002; 94:433–443. [PubMed: 12566218]
42. Cruikshank SJ, Hopperstad M, Younger M, Connors BW, Spray DC, Srinivas M. Potent block of Cx36 and Cx50 gap junction channels by mefloquine. *Proc Natl Acad Sci USA.* 2004; 101:12364–12369. [PubMed: 15297615]
43. Dahl G, Locovei S. Pannexin: to gap or not to gap, is that a question? *IUBMB Life.* 2006; 58:409–419. [PubMed: 16801216]
44. Dahm R, van Marle J, Prescott AR, Quinlan RA. Gap junctions containing alpha8-connexin (MP70) in the adult mammalian lens epithelium suggest a re-evaluation of its role in the lens. *Exp Eye Res.* 1999; 69:45–56. [PubMed: 10375448]
45. Delamere NA, Dean WL, Stidam JM, Moseley AE. Differential expression of sodium pump catalytic subunits in the lens epithelium and fibers. *Ophthalmic Res.* 1996; (28 Suppl 1):73–76. [PubMed: 8727971]
46. Delamere NA, Tamiya S. Expression, regulation and function of Na,K-ATPase in the lens. *Prog Retin Eye Res.* 2004; 23:593–615. [PubMed: 15388076]
47. DeRosa AM, Mui R, Srinivas M, White TW. Functional characterization of a naturally occurring Cx50 truncation. *Invest Ophthalmol Vis Sci.* 2006; 47:4474–4481. [PubMed: 17003442]
48. DeRosa AM, Xia CH, Gong X, White TW. The cataract-inducing S50P mutation in Cx50 dominantly alters the channel gating of wild-type lens connexins. *J Cell Sci.* 2007; 120:4107–4116. [PubMed: 18003700]
49. Devi RR, Reena C, Vijayalakshmi P. Novel mutations in GJA3 associated with autosomal dominant congenital cataract in the Indian population. *Mol Vis.* 2005; 11:846–852. [PubMed: 16254549]
50. Devi RR, Vijayalakshmi P. Novel mutations in GJA8 associated with autosomal dominant congenital cataract and microcornea. *Mol Vis.* 2006; 12:190–195. [PubMed: 16604058]
51. Donaldson P, Kistler J, Mathias RT. Molecular solutions to mammalian lens transparency. *News Physiol Sci.* 2001; 16:118–123. [PubMed: 11443230]
52. Donaldson PJ, Dong Y, Roos M, Green C, Goodenough DA, Kistler J. Changes in lens connexin expression lead to increased gap junctional voltage dependence and conductance. *Am J Physiol Cell Physiol.* 1995; 269:C590–C600.
53. Donaldson PJ, Roos M, Evans C, Beyer E, Kistler J. Electrical properties of mammalian lens epithelial gap junction channels. *Invest Ophthalmol Vis Sci.* 1994; 35:3422–3428. [PubMed: 8056517]
54. Duncan G, Colison DJ. Role of the non-neuronal cholinergic system in the eye: a review. *Life Sci.* 2003; 72:2013–2019. [PubMed: 12628451]
55. Dunia I, Cibert C, Gong X, Xia CH, Recouvreur M, Levy E, Kumar N, Bloemendal H, Benedetti EL. Structural and immunocytochemical alterations in eye lens fiber cells from Cx46 and Cx50 knockout mice. *Eur J Cell Biol.* 2006; 85:729–752. [PubMed: 16740340]
56. Dvorianchikova G, Ivanov D, Panchin Y, Shestopalov VI. Expression of pannexin family of proteins in the retina. *FEBS Lett.* 2006; 580:2178–2182. [PubMed: 16616526]

57. Ebihara L. New roles for connexins. *News Physiol Sci*. 2003; 18:100–103. [PubMed: 12750444]
58. Ebihara L, Liu X, Pal JD. Effect of external magnesium and calcium on human connexin46 hemichannels. *Biophys J*. 2003; 84:277–286. [PubMed: 12524281]
59. Ebihara L, Steiner E. Properties of a nonjunctional current expressed from a rat connexin46 cDNA in *Xenopus* oocytes. *J Gen Physiol*. 1993; 102:59–74. [PubMed: 7690837]
60. Eckert R. pH gating of lens fibre connexins. *Pflugers Arch*. 2002; 443:843–851. [PubMed: 11889584]
61. Eckert R, Donaldson P, Goldie K, Kistler J. A distinct membrane current in rat lens fiber cells isolated under calcium-free conditions. *Invest Ophthalmol Vis Sci*. 1998; 39:1280–1285. [PubMed: 9620092]
62. Evans CW, Eastwood S, Rains J, Gruijters WT, Bullivant S, Kistler J. Gap junction formation during development of the mouse lens. *Eur J Cell Biol*. 1993; 60:243–249. [PubMed: 8330621]
63. Fishman GI, Moreno AP, Spray DC, Leinwand LA. Functional analysis of human cardiac gap junction channel mutants. *Proc Natl Acad Sci USA*. 1991; 88:3525–3529. [PubMed: 1850831]
64. Francis D, Stergiopoulos K, Ek-Vitorin JF, Cao FL, Taffet SM, Delmar M. Connexin diversity and gap junction regulation by pH. *Dev Genet*. 1999; 24:123–136. [PubMed: 10079516]
65. Francis PJ, Berry V, Moore AT, Bhattacharya S. Lens biology: development and human cataractogenesis. *Trends Genet*. 1999; 15:191–196. [PubMed: 10322486]
66. Gao J, Sun X, Martinez-Wittinghan FJ, Gong X, White TW, Mathias RT. Connections between connexins, calcium, and cataracts in the lens. *J Gen Physiol*. 2004; 124:289–300. [PubMed: 15452195]
67. Gao J, Sun X, Yatsula V, Wymore RS, Mathias RT. Isoform specific function and distribution of Na/K pumps in the frog lens epithelium. *J Membr Biol*. 2000; 178:89–101. [PubMed: 11083898]
68. Gao Y, Spray DC. Structural changes in lenses of mice lacking the gap junction protein connexin43. *Invest Ophthalmol Vis Sci*. 1998; 39:1198–1209. [PubMed: 9620080]
69. Garner MH, Horowitz J. Catalytic subunit isoforms of mammalian lens Na,K-ATPase. *Curr Eye Res*. 1994; 13:65–77. [PubMed: 8156827]
70. Geering K. FXYD proteins: new regulators of Na<sup>+</sup>-K<sup>+</sup>-ATPase. *Am J Physiol Renal Physiol*. 2006; 290:F241–F250. [PubMed: 16403837]
71. Gerido DA, Sellitto C, Li L, White TW. Genetic background influences cataractogenesis, but not lens growth deficiency, in Cx50-knockout mice. *Invest Ophthalmol Vis Sci*. 2003; 44:2669–2674. [PubMed: 12766071]
72. Gerido DA, White TW. Connexin disorders of the ear, skin, and lens. *Biochim Biophys Acta*. 2004; 1662:159–170. [PubMed: 15033586]
73. Girão H, Pereira P. Phosphorylation of connexin 43 acts as a stimuli for proteasome-dependent degradation of the protein in lens epithelial cells. *Mol Vis*. 2003; 9:24–30. [PubMed: 12567182]
74. Goldberg GS, Valiunas V, Brink PR. Selective permeability of gap junction channels. *Biochim Biophys Acta*. 2004; 1662:96–101. [PubMed: 15033581]
75. Gonen T, Cheng Y, Kistler J, Walz T. Aquaporin-0 membrane junctions form upon proteolytic cleavage. *J Mol Biol*. 2004; 342:1337–1345. [PubMed: 15351655]
76. Gonen T, Sliz P, Kistler J, Cheng Y, Walz T. Aquaporin-0 membrane junctions reveal the structure of a closed water pore. *Nature*. 2004; 429:193–197. [PubMed: 15141214]
77. Gong X, Agopian K, Kumar NM, Gilula NB. Genetic factors influence cataract formation in alpha 3 connexin knockout mice. *Dev Genet*. 1999; 24:27–32. [PubMed: 10079508]
78. Gong X, Baldo GJ, Kumar NM, Gilula NB, Mathias RT. Gap junctional coupling in lenses lacking alpha3 connexin. *Proc Natl Acad Sci USA*. 1998; 95:15303–15308. [PubMed: 9860964]
79. Gong X, Cheng C, Xia CH. Connexins in lens development and cataractogenesis. *J Membr Biol*. 2007; 218:9–12. [PubMed: 17578632]
80. Gong X, Li E, Klier G, Huang Q, Wu Y, Lei H, Kumar NM, Horwitz J, Gilula NB. Disruption of alpha3 connexin gene leads to proteolysis and cataractogenesis in mice. *Cell*. 1997; 91:833–843. [PubMed: 9413992]

81. Graw J, Loster J, Soewarto D, Fuchs H, Meyer B, Reis A, Wolf E, Balling R, Hrabe DA. Characterization of a mutation in the lens-specific MP70 encoding gene of the mouse leading to a dominant cataract. *Exp Eye Res.* 2001; 73:867–876. [PubMed: 11846517]
82. Grey AC, Jacobs MD, Gonen T, Kistler J, Donaldson PJ. Insertion of MP20 into lens fibre cell plasma membranes correlates with the formation of an extracellular diffusion barrier. *Exp Eye Res.* 2003; 77:567–574. [PubMed: 14550398]
83. Griep, AE.; Zhang, P. Lens cell proliferation. In: Lovicu, FJ.; Robinson, ML., editors. *Development of the Ocular Lens.* Cambridge, UK: Cambridge Univ. Press; 2004. p. 191-213.
84. Gruijters WT, Kistler J, Bullivant S, Goodenough DA. Immunolocalization of MP70 in lens fiber 16–17-nm intercellular junctions. *J Cell Biol.* 1987; 104:565–572. [PubMed: 3818793]
85. Guleria K, Sperling K, Singh D, Varon R, Singh JR, Vanita V. A novel mutation in the connexin 46 (GJA3) gene associated with autosomal dominant congenital cataract in an Indian family. *Mol Vis.* 2007; 13:1657–1665. [PubMed: 17893674]
86. Guleria K, Vanita V, Singh D, Singh JR. A novel “pearl box” cataract associated with a mutation in the connexin 46 (GJA3) gene. *Mol Vis.* 2007; 13:797–803. [PubMed: 17615540]
87. Hamann S, Zeuthen T, La Cour M, Nagelhus EA, Ottersen OP, Agre P, Nielsen S. Aquaporins in complex tissues: distribution of aquaporins 1–5 in human and rat eye. *Am J Physiol Cell Physiol.* 1998; 274:C1332–C1345.
88. Hansen L, Yao W, Eiberg H, Funding M, Riise R, Kjaer KW, Hejtmanick JF, Rosenberg T. The congenital “ant-egg” cataract phenotype is caused by a missense mutation in connexin46. *Mol Vis.* 2006; 12:1033–1039. [PubMed: 16971895]
89. Harris AL. Emerging issues of connexin channels: biophysics fills the gap. *Q Rev Biophys.* 2001; 34:325–472. [PubMed: 11838236]
90. Ho YS, Magnenat JL, Bronson RT, Cao J, Gargano M, Sugawara M, Funk CD. Mice deficient in cellular glutathione peroxidase develop normally and show no increased sensitivity to hyperoxia. *J Biol Chem.* 1997; 272:16644–16651. [PubMed: 9195979]
91. Hopperstad MG, Srinivas M, Spray DC. Properties of gap junction channels formed by Cx46 alone and in combination with Cx50. *Biophys J.* 2000; 79:1954–1966. [PubMed: 11023900]
92. Horwitz J. Alpha-crystallin can function as a molecular chaperone. *Proc Natl Acad Sci USA.* 1992; 89:10449–10453. [PubMed: 1438232]
93. Huang YJ, Maruyama Y, Dvoryanchikov G, Pereira E, Chaudhari N, Roper SD. The role of pannexin 1 hemichannels in ATP release and cell-cell communication in mouse taste buds. *Proc Natl Acad Sci USA.* 2007; 104:6436–6441. [PubMed: 17389364]
94. Hyatt GA, Beebe DC. Regulation of lens cell growth and polarity by an embryo-specific growth factor and by inhibitors of lens cell proliferation and differentiation. *Development.* 1993; 117:701–709. [PubMed: 8330534]
95. Ireland ME, Richiert DM, Tran K. Regulation of lens beta-adrenergic receptors by receptor occupancy and dexamethasone. *J Ocul Pharmacol.* 1994; 10:543–551. [PubMed: 7836863]
96. Jacobs MD, Soeller C, Sisley AM, Cannell MB, Donaldson PJ. Gap junction processing and redistribution revealed by quantitative optical measurements of connexin46 epitopes in the lens. *Invest Ophthalmol Vis Sci.* 2004; 45:191–199. [PubMed: 14691173]
97. Jiang H, Jin Y, Bu L, Zhang W, Liu J, Cui B, Kong X, Hu L. A novel mutation in GJA3 (connexin46) for autosomal dominant congenital nuclear pulverulent cataract. *Mol Vis.* 2003; 9:579–583. [PubMed: 14627959]
98. Jiang JX, Goodenough DA. Heteromeric connexons in lens gap junction channels. *Proc Natl Acad Sci USA.* 1996; 93:1287–1291. [PubMed: 8577756]
99. Jiang JX, Paul DL, Goodenough DA. Posttranslational phosphorylation of lens fiber connexin46: a slow occurrence. *Invest Ophthalmol Vis Sci.* 1993; 34:3558–3565. [PubMed: 8258513]
100. Jiang JX, White TW, Goodenough DA. Changes in connexin expression and distribution during chick lens development. *Dev Biol.* 1995; 168:649–661. [PubMed: 7729595]
101. Kelly SM, Vanslyke JK, Musil LS. Regulation of ubiquitin-proteasome system mediated degradation by cytosolic stress. *Mol Biol Cell.* 2007; 18:4279–4291. [PubMed: 17699585]
102. King TJ, Lampe PD. Temporal regulation of connexin phosphorylation in embryonic and adult tissues. *Biochim Biophys Acta.* 2005; 1719:24–35. [PubMed: 16137642]



103. Kistler J, Bullivant S. Protein processing in lens intercellular junctions: cleavage of MP70 to MP38. *Invest Ophthalmol Vis Sci.* 1987; 28:1687–1692. [PubMed: 3654141]
104. Kistler J, Schaller J, Sigrist H. MP38 contains the membrane-embedded domain of the lens fiber gap junction protein MP70. *J Biol Chem.* 1990; 265:13357–13361. [PubMed: 2165500]
105. Konig N, Zampighi GA. Purification of bovine lens cell-to-cell channels composed of connexin44 and connexin50. *J Cell Sci.* 1995; 108:3091–3098. [PubMed: 8537448]
106. Kuszak JR, Macsai MS, Bloom KJ, Rae JL, Weinstein RS. Cell-to-cell fusion of lens fiber cells in situ: correlative light, scanning electron microscopic, and freeze-fracture studies. *J Ultrastruct Res.* 1985; 93:144–160. [PubMed: 3879764]
107. Kuszak JR, Zoltoski RK, Tiedemann CE. Development of lens sutures. *Int J Dev Biol.* 2004; 48:889–902. [PubMed: 15558480]
108. Lampe PD, Lau AF. The effects of connexin phosphorylation on gap junctional communication. *Int J Biochem Cell Biol.* 2004; 36:1171–1186. [PubMed: 15109565]
109. Lauf PK, Warwar R, Brown TL, Adragna NC. Regulation of potassium transport in human lens epithelial cells. *Exp Eye Res.* 2006; 82:55–64. [PubMed: 16002066]
110. Le AC, Musil LS. Normal differentiation of cultured lens cells after inhibition of gap junction-mediated intercellular communication. *Dev Biol.* 1998; 204:80–96. [PubMed: 9851844]
111. Le AC, Musil LS. A novel role for FGF and extracellular signal-regulated kinase in gap junction-mediated intercellular communication in the lens. *J Cell Biol.* 2001; 154:197–216. [PubMed: 11449001]
112. Li L, Lim J, Jacobs MD, Kistler J, Donaldson PJ. Regional differences in cystine accumulation point to a sutural delivery pathway to the lens core. *Invest Ophthalmol Vis Sci.* 2007; 48:1253–1260. [PubMed: 17325170]
113. Li Y, Wang J, Dong B, Man H. A novel connexin46 (GJA3) mutation in autosomal dominant congenital nuclear pulverulent cataract. *Mol Vis.* 2004; 10:668–671. [PubMed: 15448617]
114. Lim J, Lam YC, Kistler J, Donaldson PJ. Molecular characterization of the cystine/glutamate exchanger and the excitatory amino acid transporters in the rat lens. *Invest Ophthalmol Vis Sci.* 2005; 46:2869–2877. [PubMed: 16043861]
115. Lim J, Li L, Jacobs MD, Kistler J, Donaldson PJ. Mapping of glutathione and its precursor amino acids reveals a role for GLYT2 in glycine uptake in the lens core. *Invest Ophthalmol Vis Sci.* 2007; 48:5142–5151. [PubMed: 17962467]
116. Lim J, Lorentzen KA, Kistler J, Donaldson PJ. Molecular identification and characterisation of the glycine transporter (GLYT1) and the glutamine/glutamate transporter (ASCT2) in the rat lens. *Exp Eye Res.* 2006; 83:447–455. [PubMed: 16635486]
117. Lin D, Takemoto DJ. Oxidative activation of protein kinase Cgamma through the C1 domain. Effects on gap junctions. *J Biol Chem.* 2005; 280:13682–13693. [PubMed: 15642736]
118. Lin JS, Fitzgerald S, Dong Y, Knight C, Donaldson P, Kistler J. Processing of the gap junction protein connexin50 in the ocular lens is accomplished by calpain. *Eur J Cell Biol.* 1997; 73:141–149. [PubMed: 9208227]
119. Liska F, Chylikova B, Martinek J, Kren V. Microphthalmia and cataract in rats with a novel point mutation in connexin 50-L7Q. *Mol Vis.* 2008; 14:823–828. [PubMed: 18470322]
120. Liu S, Taffet S, Stoner L, Delmar M, Vallano ML, Jalife J. A structural basis for the unequal sensitivity of the major cardiac and liver gap junctions to intracellular acidification: the carboxyl tail length. *Biophys J.* 1993; 64:1422–1433. [PubMed: 8391867]
121. Lo WK, Harding CV. Square arrays and their role in ridge formation in human lens fibers. *J Ultrastruct Res.* 1984; 86:228–245. [PubMed: 6544861]
122. Lovicu, FJ.; Robinson, ML. *Development of the Ocular Lens.* Cambridge, UK: Cambridge Univ. Press; 2004.
123. Ma ZW, Zheng JQ, Li J, Li XR, Tang X, Yuan XY, Zhang XM, Sun HM. Two novel mutations of connexin genes in Chinese families with autosomal dominant congenital nuclear cataract. *Br J Ophthalmol.* 2005; 89:1535–1537. [PubMed: 16234473]
124. Mackay D, Ionides A, Kibar Z, Rouleau G, Berry V, Moore A, Shiels A, Bhattacharya S. Connexin46 mutations in autosomal dominant congenital cataract. *Am J Hum Genet.* 1999; 64:1357–1364. [PubMed: 10205266]



125. Manivannan K, Mathias RT, Gudowska-Nowak E. Description of interacting channel gating using a stochastic Markovian model. *Bull Math Biol.* 1996; 58:141–174. [PubMed: 8819758]
126. Martinez-Wittinghan FJ, Sellitto C, Li L, Gong X, Brink PR, Mathias RT, White TW. Dominant cataracts result from incongruous mixing of wild-type lens connexins. *J Cell Biol.* 2003; 161:969–978. [PubMed: 12782682]
127. Martinez-Wittinghan FJ, Sellitto C, White TW, Mathias RT, Paul D, Goodenough DA. Lens gap junctional coupling is modulated by connexin identity and the locus of gene expression. *Invest Ophthalmol Vis Sci.* 2004; 45:3629–3637. [PubMed: 15452070]
128. Martinez-Wittinghan FJ, Srinivas M, Sellitto C, White TW, Mathias RT. Mefloquine effects on the lens suggest cooperative gating of gap junction channels. *JMembr Biol.* 2006; 211:163–171. [PubMed: 17091216]
129. Mathias RT, Cohen IS, Gao J, Wang Y. Isoform-specific regulation of the Na<sup>+</sup>-K<sup>+</sup> pump in heart. *News Physiol Sci.* 2000; 15:176–180. [PubMed: 11390904]
130. Mathias RT, Kistler J, Donaldson P. The lens circulation. *J Membr Biol.* 2007; 216:1–16. [PubMed: 17568975]
131. Mathias RT, Rae JL, Baldo GJ. Physiological properties of the normal lens. *Physiol Rev.* 1997; 77:21–50. [PubMed: 9016299]
132. Mathias RT, Rae JL, Ebihara L, McCarthy RT. The localization of transport properties in the frog lens. *Biophys J.* 1985; 48:423–434. [PubMed: 3876116]
133. Mathias RT, Rae JL, Eisenberg RS. The lens as a nonuniform spherical syncytium. *Biophys J.* 1981; 34:61–83. [PubMed: 7213932]
134. Mathias RT, Riquelme G, Rae JL. Cell to cell communication and pH in the frog lens. *J Gen Physiol.* 1991; 98:1085–1103. [PubMed: 1783895]
135. Mathias RT, Wang H. Local osmosis and isotonic transport. *J Membr Biol.* 2005; 208:39–53. [PubMed: 16596445]
136. Mathias, RT.; White, TW.; Brink, PR. The role of gap junction channels in the ciliary body secretory epithelium. In: Civan, M., editor. *Current Topics in Membranes, The Eye's Aqueous Humor.* 2nd ed.. Vol. 62. Amsterdam: Elsevier; 2008. p. 71-96.chapt. 3
137. McAvoy JW, Chamberlain CG. Fibroblast growth factor (FGF) induces different responses in lens epithelial cells depending on its concentration. *Development.* 1989; 107:221–228. [PubMed: 2632221]
138. McAvoy JW, Chamberlain CG, de Longh RU, Hales AM, Lovicu FJ. Lens development. *Eye.* 1999; 13:425–437. [PubMed: 10627820]
139. McNulty R, Wang H, Mathias RT, Ortwerth BJ, Truscott RJ, Bassnett S. Regulation of tissue oxygen levels in the mammalian lens. *J Physiol.* 2004; 559:883–898. [PubMed: 15272034]
140. Menko AS. Lens epithelial cell differentiation. *Exp Eye Res.* 2002; 75:485–490. [PubMed: 12457861]
141. Merriman-Smith BR, Krushinsky A, Kistler J, Donaldson PJ. Expression patterns for glucose transporters GLUT1 and GLUT3 in the normal rat lens and in models of diabetic cataract. *Invest Ophthalmol Vis Sci.* 2003; 44:3458–3466. [PubMed: 12882795]
142. Merriman-Smith R, Donaldson P, Kistler J. Differential expression of facilitative glucose transporters GLUT1 and GLUT3 in the lens. *Invest Ophthalmol Vis Sci.* 1999; 40:3224–3230. [PubMed: 10586946]
143. Mese G, Richard G, White TW. Gap junctions: basic structure and function. *J Invest Dermatol.* 2007; 127:2516–2524. [PubMed: 17934503]
144. Miller TM, Goodenough DA. Evidence for two physiologically distinct gap junctions expressed by the chick lens epithelial cell. *J Cell Biol.* 1986; 102:194–199. [PubMed: 3079768]
145. Minogue PJ, Liu X, Ebihara L, Beyer EC, Berthoud VM. An aberrant sequence in a connexin46 mutant underlies congenital cataracts. *J Biol Chem.* 2005; 280:40788–40795. [PubMed: 16204255]
146. Moreno AP, Saez JC, Fishman GI, Spray DC. Human con-nexin43 gap junction channels. Regulation of unitary conductances by phosphorylation. *Circ Res.* 1994; 74:1050–1057. [PubMed: 7514508]

147. Moseley AE, Dean WL, Delamere NA. Isoforms of Na,K-ATPase in rat lens epithelium and fiber cells. *Invest Ophthalmol Vis Sci.* 1996; 37:1502–1508. [PubMed: 8675392]
148. Musil LS, Beyer EC, Goodenough DA. Expression of the gap junction protein connexin43 in embryonic chick lens: molecular cloning, ultrastructural localization, and post-translational phosphorylation. *J Membr Biol.* 1990; 116:163–175. [PubMed: 2166164]
149. Nielsen PA, Baruch A, Shestopalov VI, Giepmans BNG, Dunia I, Benedetti EL, Kumar NM. Lens connexins  $\alpha$ 3Cx46 and  $\alpha$ 8Cx50 interact with zonula occludens protein-1 (ZO-1). *Mol Biol Cell.* 2003; 14:2470–2481. [PubMed: 12808044]
150. Okafor M, Tamiya S, Delamere NA. Sodium-calcium exchange influences the response to endothelin-1 in lens epithelium. *Cell Calcium.* 2003; 34:231–240. [PubMed: 12887970]
151. Pal JD, Berthoud VM, Beyer EC, Mackay D, Shiels A, Ebihara L. Molecular mechanism underlying a Cx50-linked congenital cataract. *Am J Physiol Cell Physiol.* 1999; 276:C1443–C1446.
152. Pal JD, Liu X, Mackay D, Shiels A, Berthoud VM, Beyer EC, Ebihara L. Connexin46 mutations linked to congenital cataract show loss of gap junction channel function. *Am J Physiol Cell Physiol.* 2000; 279:C596–C602. [PubMed: 10942709]
153. Panchin YV. Evolution of gap junction proteins—the pannexin alternative. *J Exp Biol.* 2005; 208:1415–1419. [PubMed: 15802665]
154. Parmelee JT. Measurement of steady currents around the frog lens. *Exp Eye Res.* 1986; 42:433–441. [PubMed: 3487463]
155. Patil RV, Saito I, Wax MB. Expression of aquaporins in the rat ocular tissue. *Exp Eye Res.* 1997; 64:203–209. [PubMed: 9176054]
156. Paterson CA, Delamere NA. ATPases and lens ion balance. *Exp Eye Res.* 2004; 78:699–703. [PubMed: 15106949]
157. Paterson CA, Neville MC, Jenkins RM 2nd, Cullen JP. An electrogenic component of the potential difference in the rabbit lens. *Biochim Biophys Acta.* 1975; 375:309–316. [PubMed: 1125214]
158. Paul DL, Ebihara L, Takemoto LJ, Swenson KI, Goodenough DA. Connexin46, a novel lens gap junction protein, induces voltage-gated currents in nonjunctional plasma membrane of *Xenopus* oocytes. *J Cell Biol.* 1991; 115:1077–1089. [PubMed: 1659572]
159. Pelegrin P, Surprenant A. Pannexin-1 mediates large pore formation and interleukin-1beta release by the ATP-gated P2 $\times$ 7 receptor. *EMBO J.* 2006; 25:5071–5082. [PubMed: 17036048]
160. Penuela S, Bhalla R, Gong XQ, Cowan KN, Celetti SJ, Cowan BJ, Bai D, Shao Q, Laird DW. Pannexin 1 and pannexin 3 are glycoproteins that exhibit many distinct characteristics from the connexin family of gap junction proteins. *J Cell Sci.* 2007; 120:3772–3783. [PubMed: 17925379]
161. Piatigorsky J. Lens differentiation in vertebrates. A review of cellular and molecular features. *Differentiation.* 1981; 19:134–153. [PubMed: 7030840]
162. Polyakov AV, Shagina IA, Khlebnikova OV, Evgrafov OV. Mutation in the connexin 50 gene (GJA8) in a Russian family with zonular pulverulent cataract. *Clin Genet.* 2001; 60:476–478. [PubMed: 11846744]
163. Ponnamp SP, Ramesha K, Tejwani S, Ramamurthy B, Kannabiran C. Mutation of the gap junction protein alpha 8 (GJA8) gene causes autosomal recessive cataract. *J Med Genet.* 2007; 44:e85. [PubMed: 17601931]
164. Preston GM, Agre P. Isolation of the cDNA for erythrocyte integral membrane protein of 28 kilodaltons: member of an ancient channel family. *Proc Natl Acad Sci USA.* 1991; 88:11110–11114. [PubMed: 1722319]
165. Rae JL, Bartling C, Rae J, Mathias RT. Dye transfer between cells of the lens. *J Membr Biol.* 1996; 150:89–103. [PubMed: 8699483]
166. Rae JL, Mathias RT, Cooper K, Baldo G. Divalent cation effects on lens conductance and stretch-activated cation channels. *Exp Eye Res.* 1992; 55:135–144. [PubMed: 1383018]
167. Reaume AG, de Sousa PA, Kulkarni S, Langille BL, Zhu D, Davies TC, Juneja SC, Kidder GM, Rossant J. Cardiac malformation in neonatal mice lacking connexin43. *Science.* 1995; 267:1831–1834. [PubMed: 7892609]

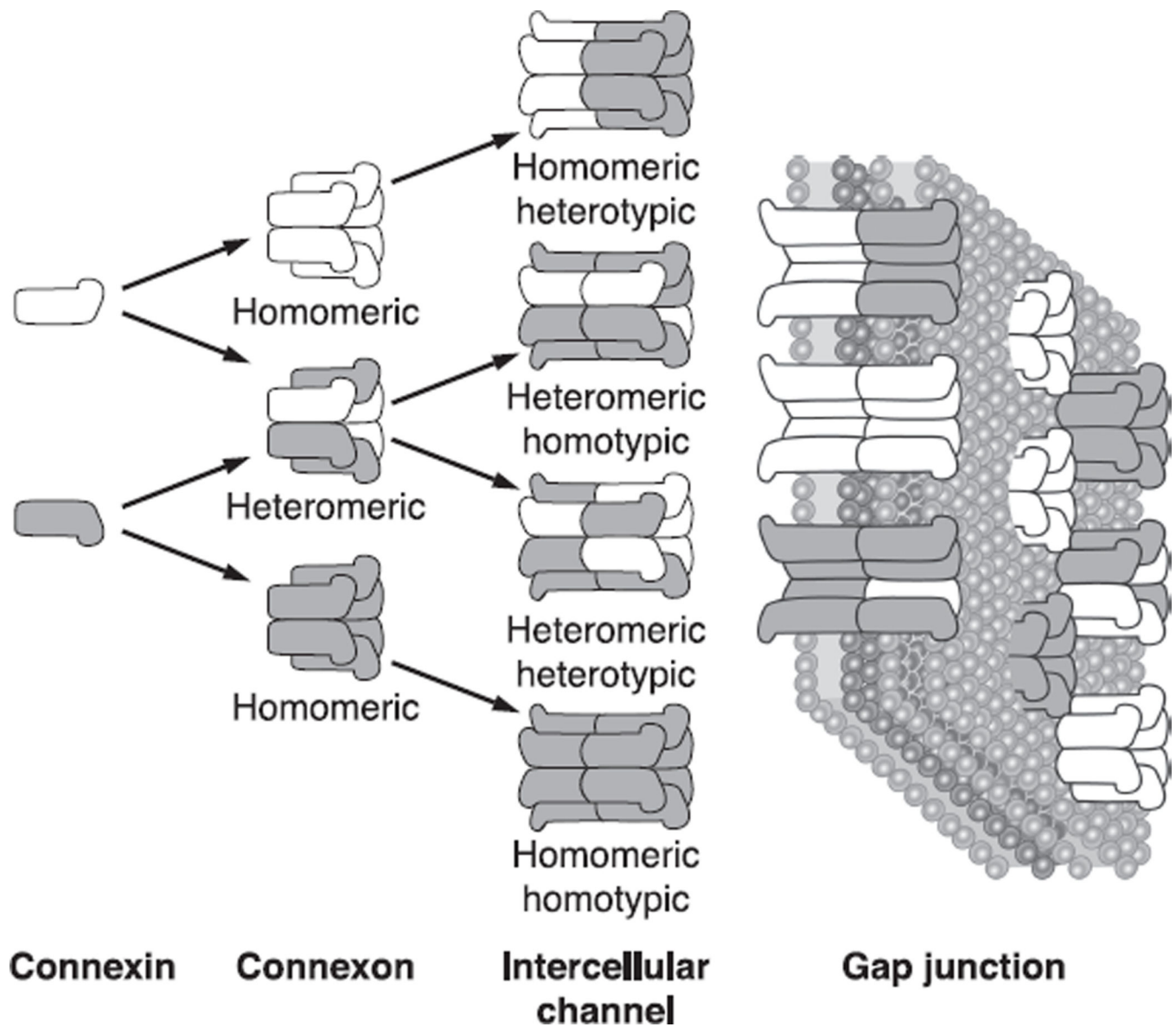
168. Rees MI, Watts P, Fenton I, Clarke A, Snell RG, Owen MJ, Gray J. Further evidence of autosomal dominant congenital zonular pulverulent cataracts linked to 13q11 (CZP3) and a novel mutation in connexin 46 (GJA3). *Hum Genet.* 2000; 106:206–209. [PubMed: 10746562]
169. Reddy VN, Giblin FJ, Lin LR, Dang L, Unakar NJ, Musch DC, Boyle DL, Takemoto LJ, Ho YS, Knoernschild T, Juenemann A, Lütjen-Drecoll E. Glutathione peroxidase-1 deficiency leads to increased nuclear light scattering, membrane damage, and cataract formation in gene-knockout mice. *Invest Ophthalmol Vis Sci.* 2001; 42:3247–3255. [PubMed: 11726630]
170. Revel JP, Karnovsky MJ. Hexagonal array of subunits in intercellular junctions of the mouse heart and liver. *J Cell Biol.* 1967; 33:C7–C12. [PubMed: 6036535]
171. Robinson KR, Paterson JW. Localization of steady currents in the lens. *Curr Eye Res.* 1982; 2:843–847. [PubMed: 7187641]
172. Rong P, Wang X, Niesman Wu Y, Benedetti LE, Dunia I, Levy E, Gong X. Disruption of Gja8 (alpha8 connexin) in mice leads to microphthalmia associated with retardation of lens growth and lens fiber maturation. *Development.* 2002; 129:167–174. [PubMed: 11782410]
173. Ruiz-Ederra J, Verkman AS. Accelerated cataract formation and reduced lens epithelial water permeability in aquaporin-1-deficient mice. *Invest Ophthalmol Vis Sci.* 2006; 47:3960–3967. [PubMed: 16936111]
174. Runge PE, Hawes NL, Heckenlively JR, Langley SH, Roderick TH. Autosomal dominant mouse cataract (Lop-10). Consistent differences of expression in heterozygotes. *Invest Ophthalmol Vis Sci.* 1992; 33:3202–3208. [PubMed: 1399425]
175. Schmidt W, Klopp N, Illig T, Graw J. A novel GJA8 mutation causing a recessive triangular cataract. *Mol Vis.* 2008; 14:851–856. [PubMed: 18483562]
176. Schuetze SM, Goodenough DA. Dye transfer between cells of the embryonic chick lens becomes less sensitive to CO<sub>2</sub> treatment with development. *J Cell Biol.* 1982; 92:694–705. [PubMed: 6806303]
177. Sellitto C, Li L, White TW. Connexin50 is essential for normal postnatal lens cell proliferation. *Invest Ophthalmol Vis Sci.* 2004; 45:3196–3202. [PubMed: 15326140]
178. Shepard AR, Rae JL. Ion transporters and receptors in cDNA libraries from lens and cornea epithelia. *Curr Eye Res.* 1998; 17:708–719. [PubMed: 9678416]
179. Shestopalov VI, Panchin Y. Pannexins and gap junction protein diversity. *Cell Mol Life Sci.* 2008; 65:376–394. [PubMed: 17982731]
180. Shi Y, Barton K, De Maria A, Petrash JM, Shiels A, Bassnett S. The stratified syncytium of the vertebrate lens. *J Cell Sci.* 2009; 122:1607–1615. [PubMed: 19401333]
181. Shiels A, Bassnett S, Varadaraj K, Mathias R, Al-Ghoul K, Kuszak J, Donoviel D, Lilleberg S, Friedrich G, Zambrowicz B. Optical dysfunction of the crystalline lens in aquaporin-0-deficient mice. *Physiol Gen.* 2001; 7:179–186.
182. Shiels A, Mackay D, Ionides A, Berry V, Moore A, Bhattacharya S. A missense mutation in the human connexin50 gene (GJA8) underlies autosomal dominant “zonular pulverulent” cataract, on chromosome 1q. *Am J Hum Genet.* 1998; 62:526–532. [PubMed: 9497259]
183. Shui YB, Fu JJ, Garcia C, Dattilo LK, Rajagopal R, McMillan S, Mak G, Holekamp NM, Lewis A, Beebe DC. Oxygen distribution in the rabbit eye and oxygen consumption by the lens. *Invest Ophthalmol Vis Sci.* 2006; 47:1571–1580. [PubMed: 16565394]
184. Srinivas M, Costa M, Gao Y, Fort A, Fishman GI, Spray DC. Voltage dependence of macroscopic and unitary currents of gap junction channels formed by mouse connexin50 expressed in rat neuroblastoma cells. *J Physiol.* 1999; 517:673–689. [PubMed: 10358109]
185. Srinivas M, Hopperstad MG, Spray DC. Quinine blocks specific gap junction channel subtypes. *Proc Natl Acad Sci USA.* 2001; 98:10942–10947. [PubMed: 11535816]
186. Srivastava SK, Wang LF, Ansari NH, Bhatnagar A. Calcium homeostasis of isolated single cortical fibers of rat lens. *Invest Ophthalmol Vis Sci.* 1997; 38:2300–2312. [PubMed: 9344353]
187. Steele EC Jr, Lyon MF, Favor J, Guillot NPV, Boyd Y, Church RL. A mutation in the connexin 50 (Cx50) gene is a candidate for the No2 mouse cataract. *Curr Eye Res.* 1998; 17:883–889. [PubMed: 9746435]

188. Stergiopoulos K, Alvarado JL, Mastroianni M, Ek-Vitorin JF, Taffet SM, Delmar M. Hetero-domain interactions as a mechanism for the regulation of connexin channels. *Circ Res.* 1999; 84:1144–1155. [PubMed: 10347089]
189. Sweadner KJ. Isozymes of the Na<sup>+</sup>/K<sup>+</sup>-ATPase. *Biochim Biophys Acta.* 1989; 988:185–220. [PubMed: 2541792]
190. Swenson KI, Jordan JR, Beyer EC, Paul DL. Formation of gap junctions by expression of connexins in *Xenopus* oocyte pairs. *Cell.* 1989; 57:145–155. [PubMed: 2467743]
191. Tamiya S, Dean WL, Paterson CA, Delamere NA. Regional distribution of Na,K-ATPase activity in porcine lens epithelium. *Invest Ophthalmol Vis Sci.* 2003; 44:4395. [PubMed: 14507885]
192. Tamiya S, Delamere NA. The influence of sodium-calcium exchange inhibitors on rabbit lens ion balance and transparency. *Exp Eye Res.* 2006; 83:1089–1095. [PubMed: 16839544]
193. Tang Y, Liu X, Zoltoski RK, Novak LA, Herrera RA, Richard I, Kuszak JR, Kumar NM. Age-related cataracts in alpha3 Cx46-knockout mice are dependent on a calpain 3 isoform. *Invest Ophthalmol Vis Sci.* 2007; 48:2685–2694. [PubMed: 17525200]
194. Varadaraj K, Kumari SS, Mathias RT. Functional expression of aquaporins in embryonic, postnatal, and adult mouse lenses. *Dev Dyn.* 2007; 236:1319–1328. [PubMed: 17377981]
195. Varadaraj K, Kumari S, Shiels A, Mathias RT. Regulation of aquaporin water permeability in the lens. *Invest Ophthalmol Vis Sci.* 2005; 46:1393–1402. [PubMed: 15790907]
196. Varadaraj K, Kushmerick C, Baldo GJ, Bassnett S, Shiels A, Mathias RT. The role of MIP in lens fiber cell membrane transport. *J Membr Biol.* 1999; 170:191–203. [PubMed: 10441663]
197. Valiunas V, Beyer EC, Brink PR. Cardiac gap junction channels show quantitative differences in selectivity. *Circ Res.* 2002; 91:104–111. [PubMed: 12142342]
198. Vanden Abeele F, Bidaux G, Gordienko D, Beck B, Panchin YV, Baranova AV, Ivanov DV, Skryma R, Prevarskaya N. Functional implications of calcium permeability of the channel formed by pannexin 1. *J Cell Biol.* 2006; 174:535–546. [PubMed: 16908669]
199. Vanita V, Hennies HC, Singh D, Nurnberg P, Sperling K, Singh JR. A novel mutation in GJA8 associated with autosomal dominant congenital cataract in a family of Indian origin. *Mol Vis.* 2006; 12:1217–1222. [PubMed: 17110920]
200. Vanita V, Singh JR, Singh D, Varon R, Sperling K. A mutation in GJA8 (p.P88Q) is associated with “balloon-like” cataract with Y-sutural opacities in a family of Indian origin. *Mol Vis.* 2008; 14:1171–1175. [PubMed: 18587493]
201. Vanita V, Singh JR, Singh D, Varon R, Sperling K. A novel mutation in GJA8 associated with jellyfish-like cataract in a family of Indian origin. *Mol Vis.* 2008; 14:323–326. [PubMed: 18334946]
202. Verkman AS. Role of aquaporin water channels in kidney and lung. *Am J Med Sci.* 1998; 316:310–320. [PubMed: 9822113]
203. Voorter CE, Kistler J. cAMP-dependent protein kinase phosphorylates gap junction protein in lens cortex but not in lens nucleus. *Biochim Biophys Acta.* 1989; 986:8–10. [PubMed: 2554983]
204. Wang H, Gao J, Sun X, Martinez-Wittinghan FJ, Li L, Varadaraj K, Farrell M, Reddy VN, White TW, Mathias RT. The effects of GPX-1 knockout on membrane transport and intracellular homeostasis in the lens. *J Membr Biol.* 2009; 227:25–37. [PubMed: 19067024]
205. Wang J, Ma M, Locovei S, Keane RW, Dahl G. Modulation of membrane channel currents by gap junction protein mimetic peptides: size matters. *Am J Physiol Cell Physiol.* 2007; 293:C1112–C1119. [PubMed: 17652431]
206. Wang LF, Dhir P, Bhatnagar A, Srivastava SK. Contribution of osmotic changes to disintegrative globulization of single cortical fibers isolated from rat lens. *Exp Eye Res.* 1997; 65:267–275. [PubMed: 9268595]
207. Wang Z, Han J, Schey KL. Spatial differences in an integral membrane proteome detected in laser capture microdissected samples. *J Proteome Res.* 2008; 7:2696–2702. [PubMed: 18489132]
208. Webb K, Donaldson PJ. Differentiation-dependent changes in the membrane properties of fiber cells isolated from the rat lens. *Am J Physiol Cell Physiol.* 2008; 294:C1133–C1145. [PubMed: 18367590]

209. Webb KF, Merriman-Smith BR, Stobie JK, Kistler J, Donaldson PJ.  $\text{Cl}^-$  influx into rat cortical lens fiber cells is mediated by a  $\text{Cl}^-$  conductance that is not  $\text{ClC-2}$  or  $-3$ . *Invest Ophthalmol Vis Sci.* 2004; 45:4400–4408. [PubMed: 15557448]
210. White TW. Unique and redundant connexin contributions to lens development. *Science.* 2002; 295:319–320. [PubMed: 11786642]
211. White TW. Nonredundant gap junction functions. *News Physiol Sci.* 2003; 18:95–99. [PubMed: 12750443]
212. White TW, Bruzzone R, Goodenough DA, Paul DL. Mouse Cx50, a functional member of the connexin family of gap junction proteins, is the lens fiber protein MP70. *Mol Biol Cell.* 1992; 3:711–720. [PubMed: 1325220]
213. White TW, Bruzzone R, Paul DL. The connexin family of intercellular channel forming proteins. *Kidney Int.* 1995; 48:1148–1157. [PubMed: 8569076]
214. White TW, Bruzzone R, Wolfram S, Paul DL, Goodenough DA. Selective interactions among the multiple connexin proteins expressed in the vertebrate lens: the second extracellular domain is a determinant of compatibility between connexins. *J Cell Biol.* 1994; 125:879–892. [PubMed: 8188753]
215. White TW, Gao Y, Li L, Sellitto C, Srinivas M. Optimal lens epithelial cell proliferation is dependent on the connexin isoform providing gap junctional coupling. *Invest Ophthalmol Vis Sci.* 2007; 48:5630–5637. [PubMed: 18055813]
216. White TW, Goodenough DA, Paul DL. Targeted ablation of connexin50 in mice results in microphthalmia and zonular pulverulent cataracts. *J Cell Biol.* 1998; 143:815–825. [PubMed: 9813099]
217. White TW, Paul DL. Genetic diseases and gene knockouts reveal diverse connexin functions. *AnnuRev Physiol.* 1999; 61:283–310.
218. White TW, Wang H, Mui R, Litteral J, Brink PR. Cloning and functional expression of invertebrate connexins from *Halocynthia pyriformis*. *FEBS Lett.* 2004; 577:42–48. [PubMed: 15527759]
219. Williams MR, Duncan G, Croghan PC, Riach R, Webb SF. pH regulation in tissue-cultured bovine lens epithelial cells. *J Membr Biol.* 1992; 129:179–187. [PubMed: 1331465]
220. Willoughby CE, Arab S, Gandhi R, Zeinali S, Luk D, Billings-ley G, Munier FL, Heon E. A novel GJA8 mutation in an Iranian family with progressive autosomal dominant congenital nuclear cataract. *J Med Genet.* 2003; 40:e124. [PubMed: 14627691]
221. Wolosin JM, Alvarez LJ, Candia OA. Cellular pH and  $\text{Na}^+\text{-H}^+$  exchange activity in lens epithelium of *Bufo marinus* toad. *Am J Physiol.* 1988; 255:C595–C602. [PubMed: 2847535]
222. Xia CH, Cheng C, Huang Q, Cheung D, Li L, Dunia I, Benedetti LE, Horwitz J, Gong X. Absence of alpha3 (Cx46) and alpha8 (Cx50) connexins leads to cataracts by affecting lens inner fiber cells. *Exp Eye Res.* 2006; 83:688–696. [PubMed: 16696970]
223. Xia CH, Cheung D, DeRosa AM, Chang B, Lo WK, White TW, Gong X. Knock-in of alpha3 connexin prevents severe cataracts caused by an alpha8 point mutation. *J Cell Sci.* 2006; 119:2138–2144. [PubMed: 16687738]
224. Xia CH, Liu H, Cheung D, Cheng C, Wang E, Du X, Beutler B, Lo WK, Gong X. Diverse gap junctions modulate distinct mechanisms for fiber cell formation during lens development and cataractogenesis. *Development.* 2006; 133:2033–2040. [PubMed: 16611690]
225. Xu X, Ebihara L. Characterization of a mouse Cx50 mutation associated with the No2 mouse cataract. *Invest Ophthalmol Vis Sci.* 1999; 40:1844–1850. [PubMed: 10393059]
226. Yamashita S, Furumoto K, Nobukiyo A, Kamohara M, Ushijima T, Furukawa T. Mapping of A gene responsible for cataract formation and its modifier in the UPL rat. *Invest Ophthalmol Vis Sci.* 2002; 43:3153–3159. [PubMed: 12356818]
227. Yan M, Xiong C, Ye SQ, Chen Y, Ke M, Zheng F, Zhou X. A novel connexin 50 (GJA8) mutation in a Chinese family with a dominant congenital pulverulent nuclear cataract. *Mol Vis.* 2008; 14:418–424. [PubMed: 18334966]
228. Yancey SB, Biswal S, Revel JP. Spatial and temporal patterns of distribution of the gap junction protein connexin43 during mouse gastrulation and organogenesis. *Development.* 1992; 114:203–212. [PubMed: 1315676]

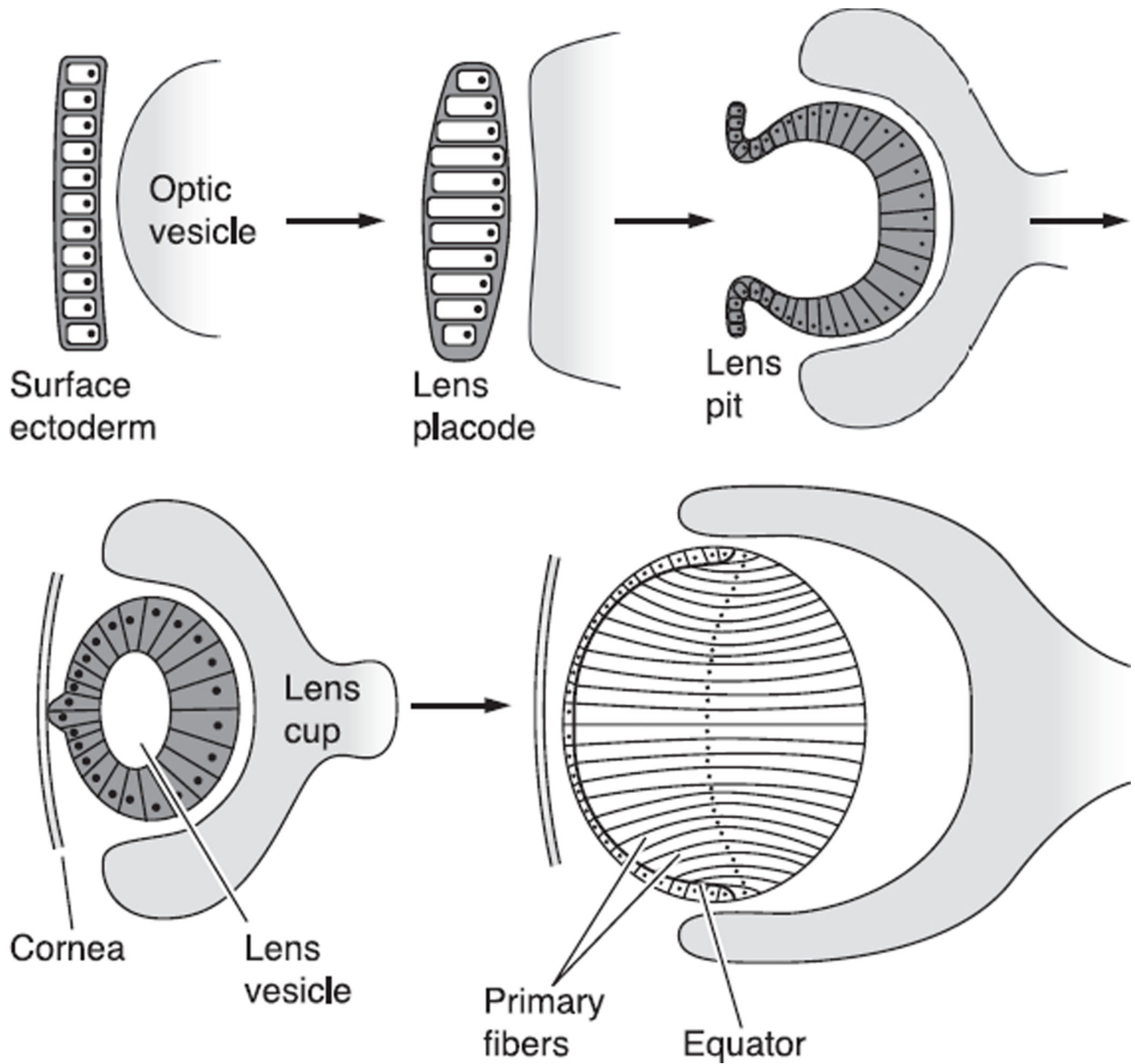
229. Ye JJ, Zadunaisky JA. A Na<sup>+</sup>/H<sup>+</sup> exchanger and its relation to oxidative effects in plasma membrane vesicles from lens fibers. *Exp Eye Res.* 1992; 55:251–260. [PubMed: 1330662]
230. Yeager M, Harris AL. Gap junction channel structure in the early 21st century: facts and fantasies. *Curr Opin Cell Biol.* 2007; 19:521–528. [PubMed: 17945477]
231. Yoshida M, Harada Y, Kaidzu S, Ohira A, Masuda J, Nabika T. New genetic model rat for congenital cataracts due to a connexin 46 (Gja3) mutation. *Pathol Int.* 2005; 55:732–737. [PubMed: 16271086]
232. Zampighi GA, Eskandari S, Kreman M. Epithelial organization of the mammalian lens. *Exp Eye Res.* 2000; 71:415–435. [PubMed: 10995562]
233. Zampighi GA, Hall JE, Ehrling GR, Simon SA. The structural organization and protein composition of lens fiber junctions. *J Cell Biol.* 1989; 108:2255–2275. [PubMed: 2738093]
234. Zampighi GA, Planells AM, Lin D, Takemoto D. Regulation of lens cell-to-cell communication by activation of PKC $\gamma$  and disassembly of Cx50 channels. *Invest Ophthalmol Vis Sci.* 2005; 46:3247–3255. [PubMed: 16123426]
235. Zampighi GA, Simon SA, Hall JE. The specialized junctions of the lens. *Int Rev Cytol.* 1992; 136:185–225. [PubMed: 1506144]
236. Zatechka SD Jr, Lou MF. Studies of the mitogen-activated protein kinases and phosphatidylinositol-3 kinase in the lens. 1. The mitogenic and stress responses. *Exp Eye Res.* 2002; 74:703–717. [PubMed: 12126944]
237. Zhang W, Zitron E, Homme M, Kihm L, Morath C, Scherer D, Hegge S, Thomas D, Schmitt CP, Zeier M, Katus H, Karle C, Schwenger V. Aquaporin-1 channel function is positively regulated by protein kinase C. *J Biol Chem.* 2007; 282:20933–20940. [PubMed: 17522053]
238. Zheng JQ, Ma ZW, Sun HM. A heterozygous transversion of connexin 50 in a family with congenital nuclear cataract in the northeast of China. *Zhonghua Yi Xue Yi Chuan Xue Za Zhi.* 2005; 22:76–78. [PubMed: 15696487]



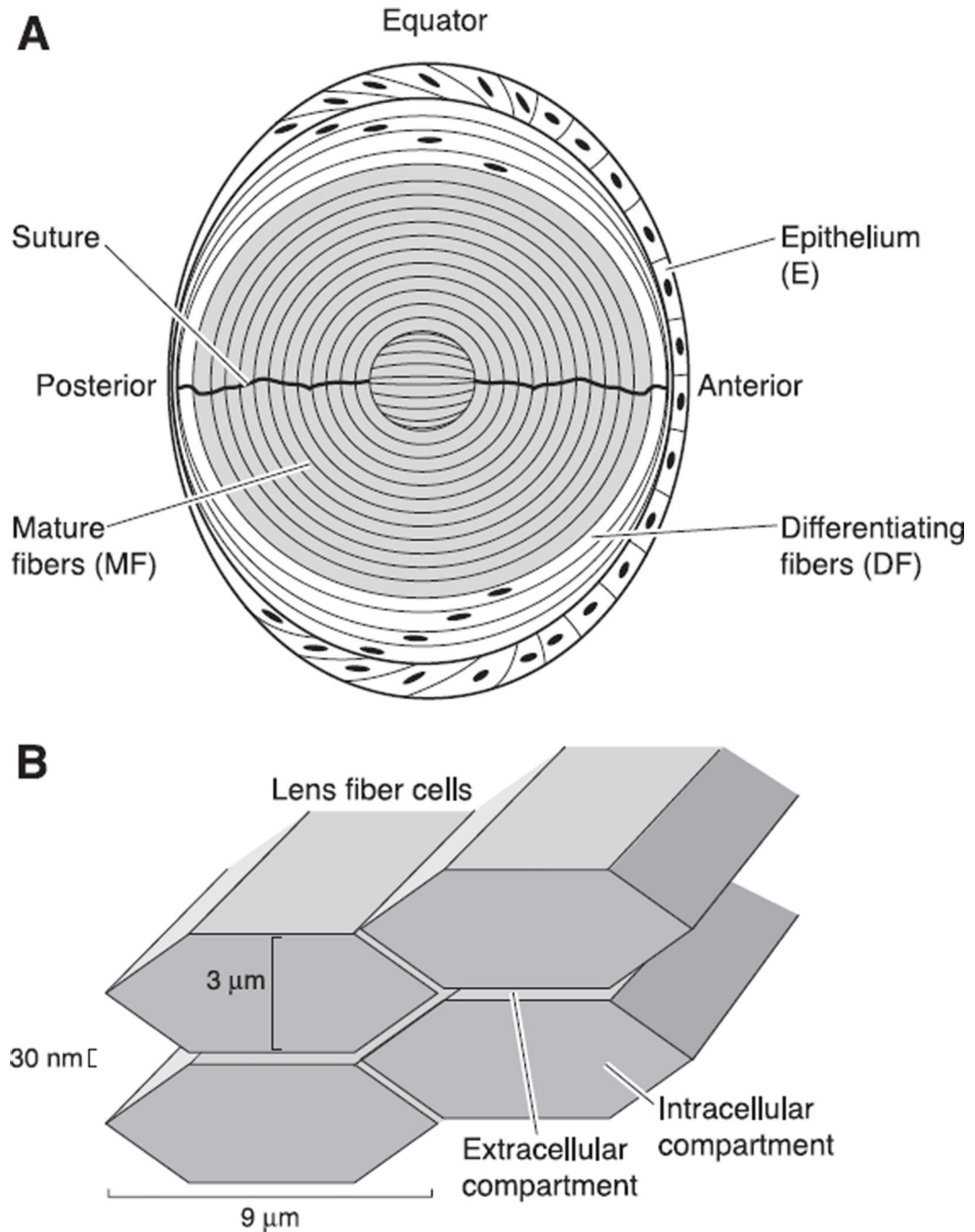


**Fig. 1.**

The nomenclature for the different types of intercellular channels that can form a gap junction. The gap junction comprises many closely packed cell-to-cell channels connecting the cytoplasm of adjacent cells. Each channel is formed by the docking of two hemichannels, or connexons, one in each of the two cells. Each hemichannel is composed of six subunit connexins. The connexin family of proteins includes many isoforms that can intermix to form hemichannels and intact channels, as shown in the figure.



**Fig. 2.** The stages of development of the embryonic lens starting from formation of the surface ectoderm and leading to formation of the initial identifiable lens, which has only primary fibers. [From Francis et al. (65), with permission from Elsevier Science.]

**Fig. 3.**

The structure of the mature lens. *A*: a sketch of the cellular structure of the lens. As described in the text, the transport properties of lens cells differ in three zones. The epithelium, which caps the front of the lens, expresses most of the active transport proteins in the lens. The mature fibers, which contain no organelles, fill the majority of the volume of the lens. They express membrane transporters for nutrients and antioxidants that are needed for homeostasis. Between the epithelium and mature fibers are the differentiating fibers, which still have organelles, but have different membrane transporters than the epithelium. *B*:

the structure of the intracellular and extracellular compartments within the lens. When cut in cross-section (an equatorial section of the structure shown in *A*), the lens fibers are flattened hexagons of the approximate dimensions shown. The extracellular and intracellular compartments communicate through transporters in the fiber cell membranes.

Author Manuscript

Author Manuscript

Author Manuscript

Author Manuscript

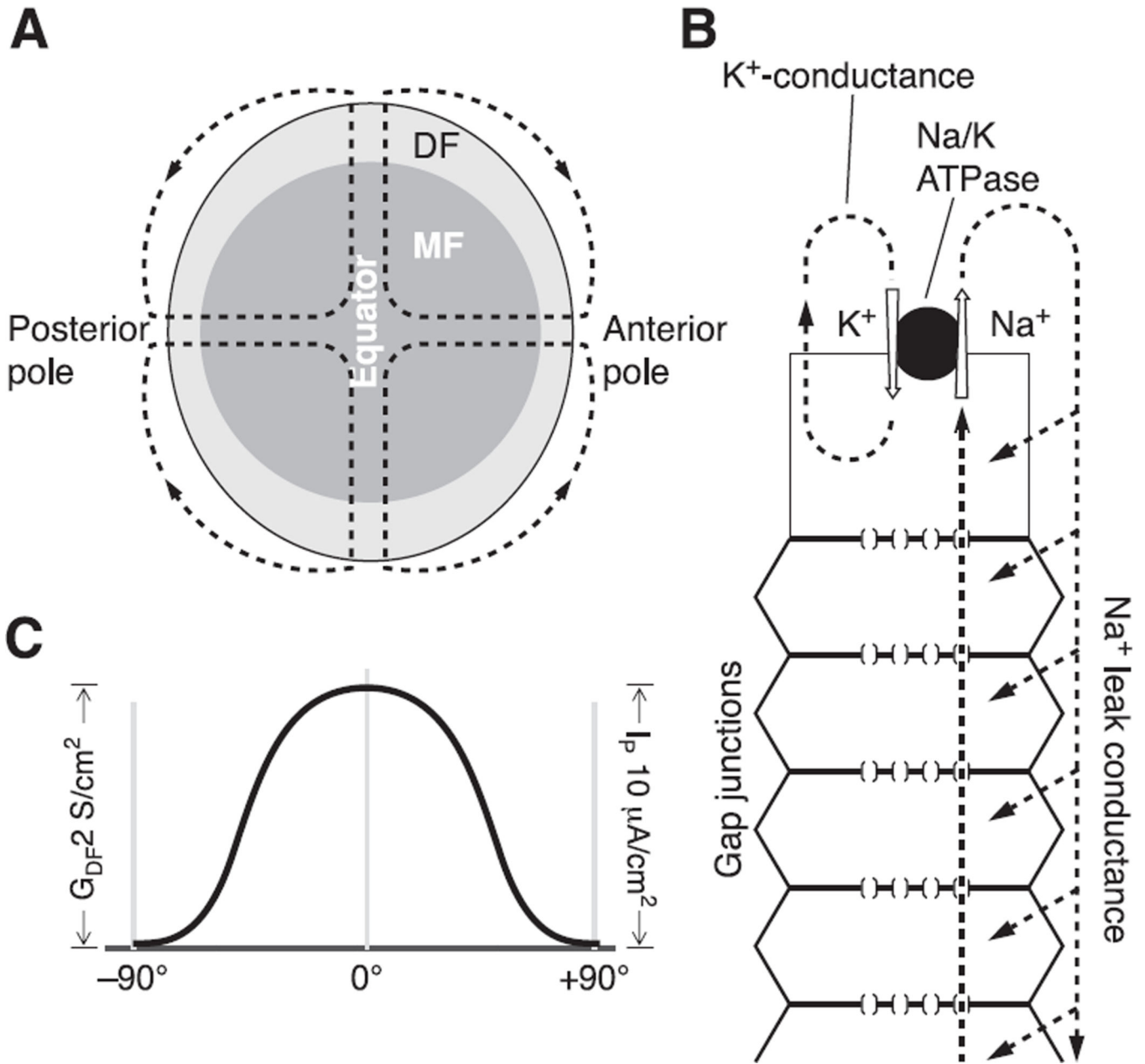


**Fig. 4.**

The lens circulation. *A*: circulating currents enter the lens at both poles and exit at the equator. This panel indicates the overall pattern of current flow without regard to detail. *B*: a more detailed sketch of how the currents enter and exit the lens. The inward currents, which are carried by Na<sup>+</sup>, enter the lens along the extracellular spaces. The outward currents, which are also carried by Na<sup>+</sup>, are intracellular, flowing from cell to cell through gap junctions to reach the epithelium, where the Na<sup>+</sup>-K<sup>+</sup> pumps transport the Na<sup>+</sup> out of the lens to complete the current loops. The spatial separation of active Na<sup>+</sup> extrusion from passive Na<sup>+</sup> entry creates the circulation from surface to interior but does not explain the complex pattern. *C*: the factors responsible for the complex pattern of flow. Gap junction coupling

conductance is concentrated in the equatorial region of differentiating fibers (DF), thus directing the outward intracellular flow to the equatorial epithelial cells, where  $\text{Na}^+\text{-K}^+$  pump expression per unit area of lens surface is highly concentrated to transport the  $\text{Na}^+$  out at the equator. [From Mathias et al. (130), with permission from Springer Science + Business Media.]

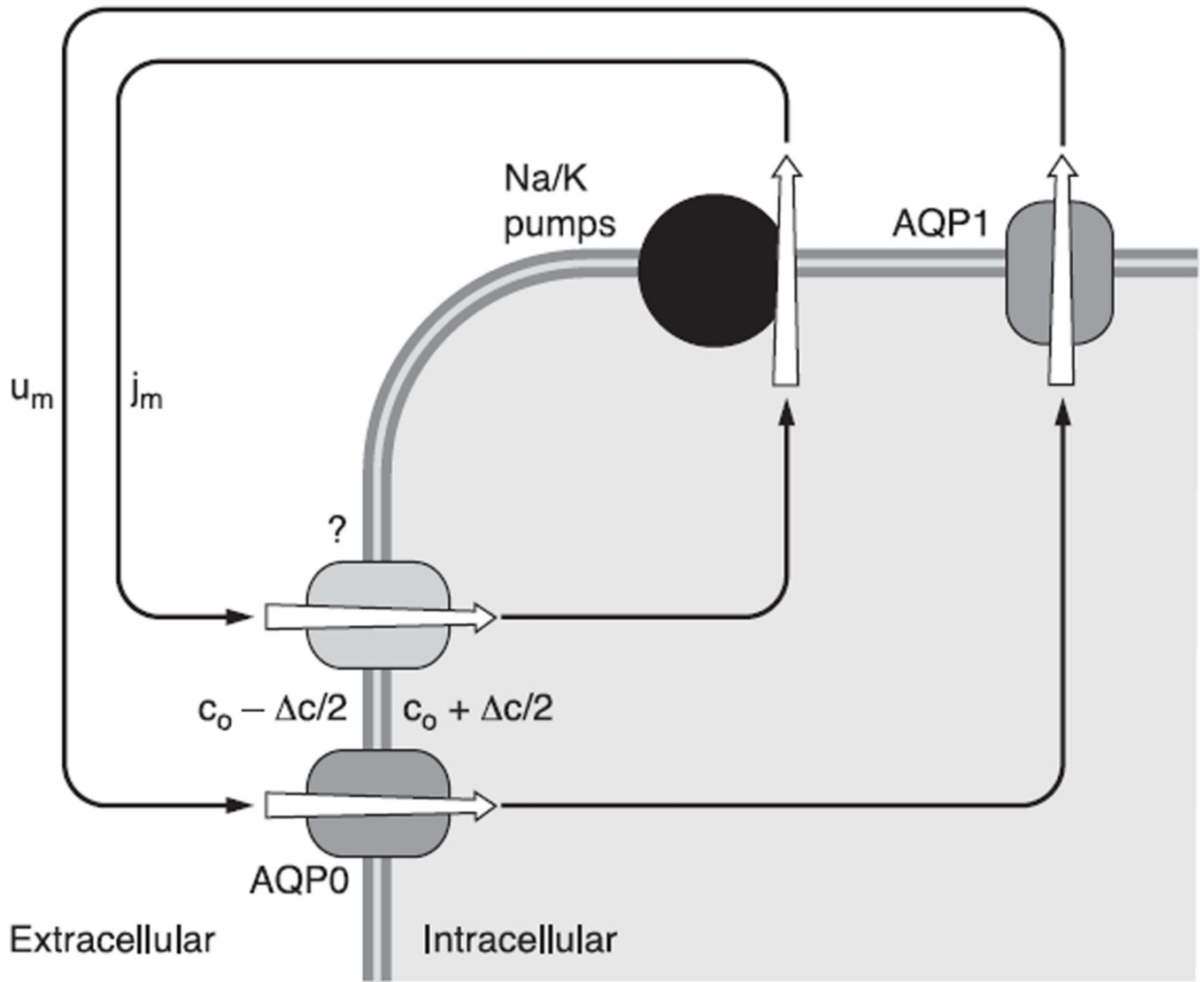
Author Manuscript

Author Manuscript

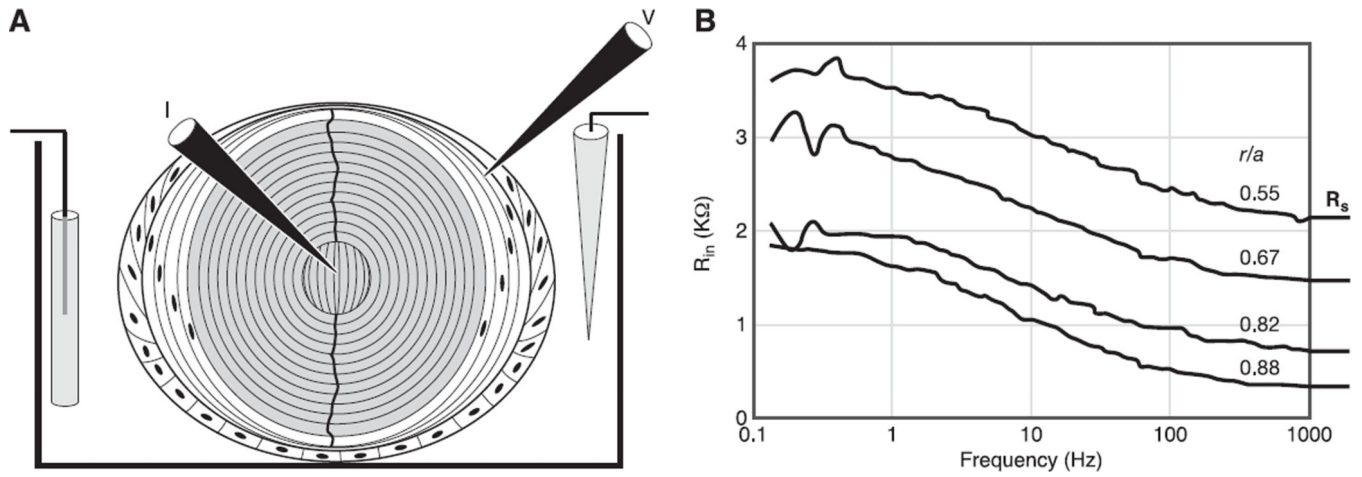
Author Manuscript

Author Manuscript



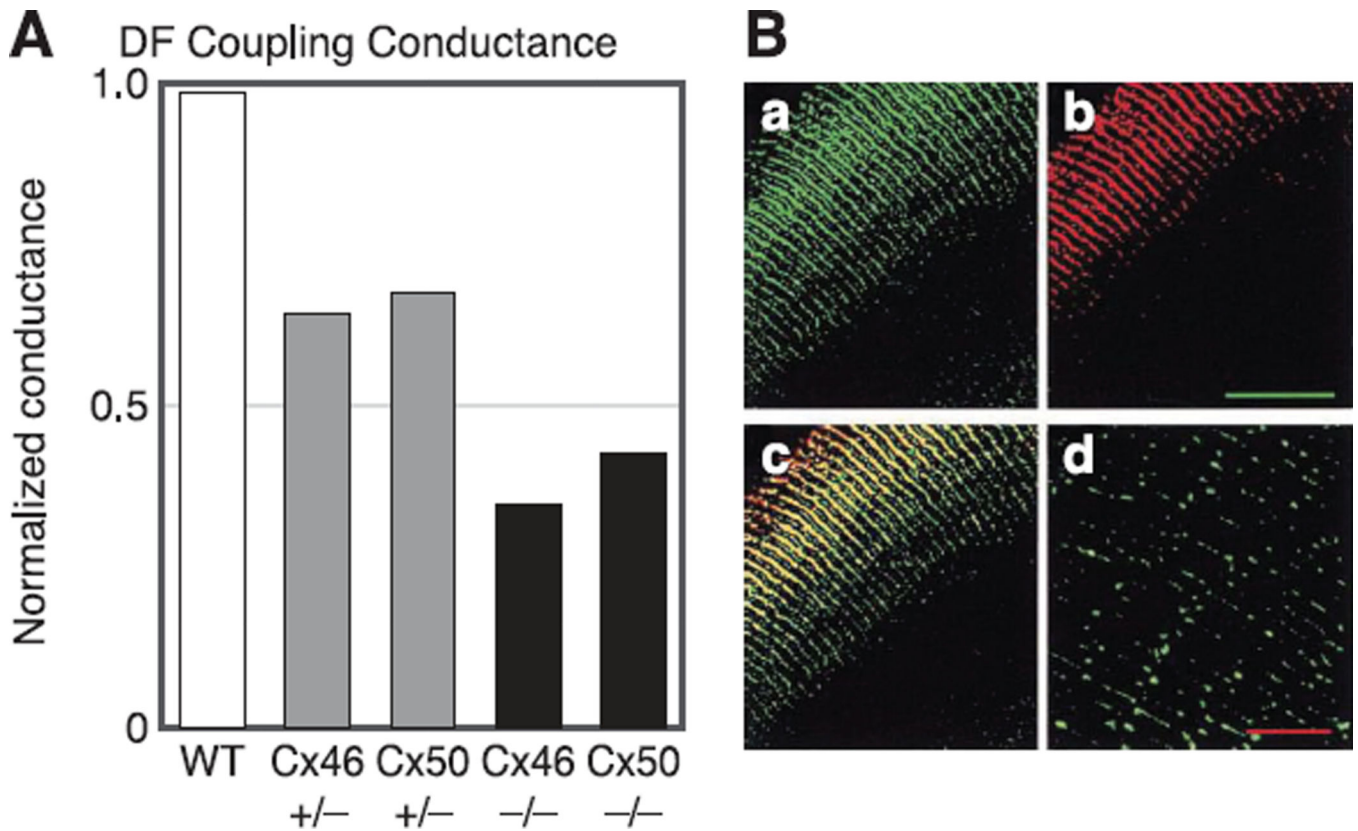


**Fig. 5.** The coupling through local osmosis of the circulating flow of solute ( $j_m$ ) to a circulation of fluid ( $u_m$ ). In this model, circulating  $\text{Na}^+$  current creates a circulation of solute that drives fluid to move in the same pattern. The complex pattern ensures the fluid is well stirred and can carry fresh nutrients and antioxidants into the lens along the extracellular spaces to the central fiber cells, which are too far from the lens surface for diffusion to be effective. Thus the avascular lens generates its own internal microcirculatory system. [From Mathias et al. (130), with permission from Springer Science + Business Media.]

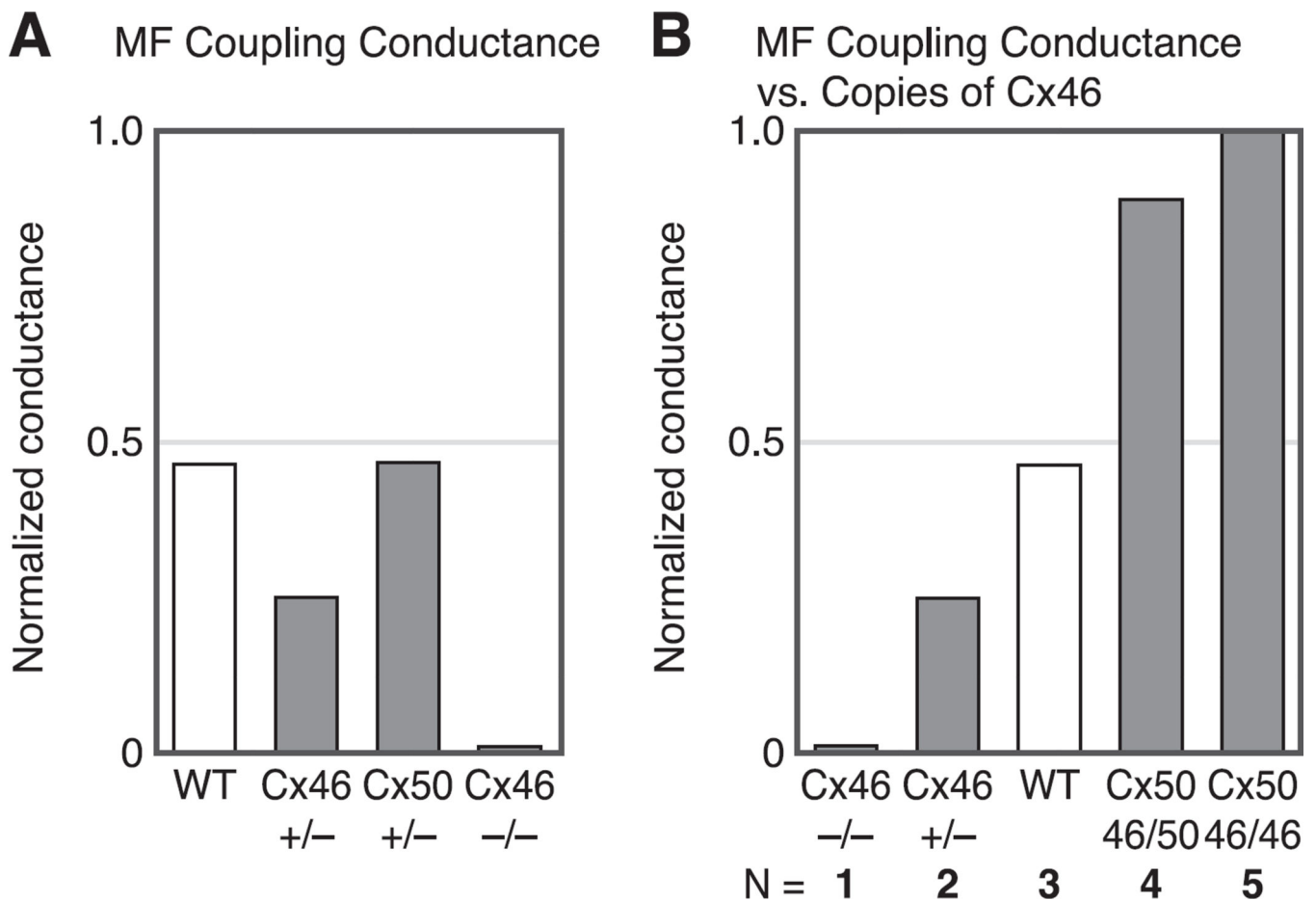


**Fig. 6.**

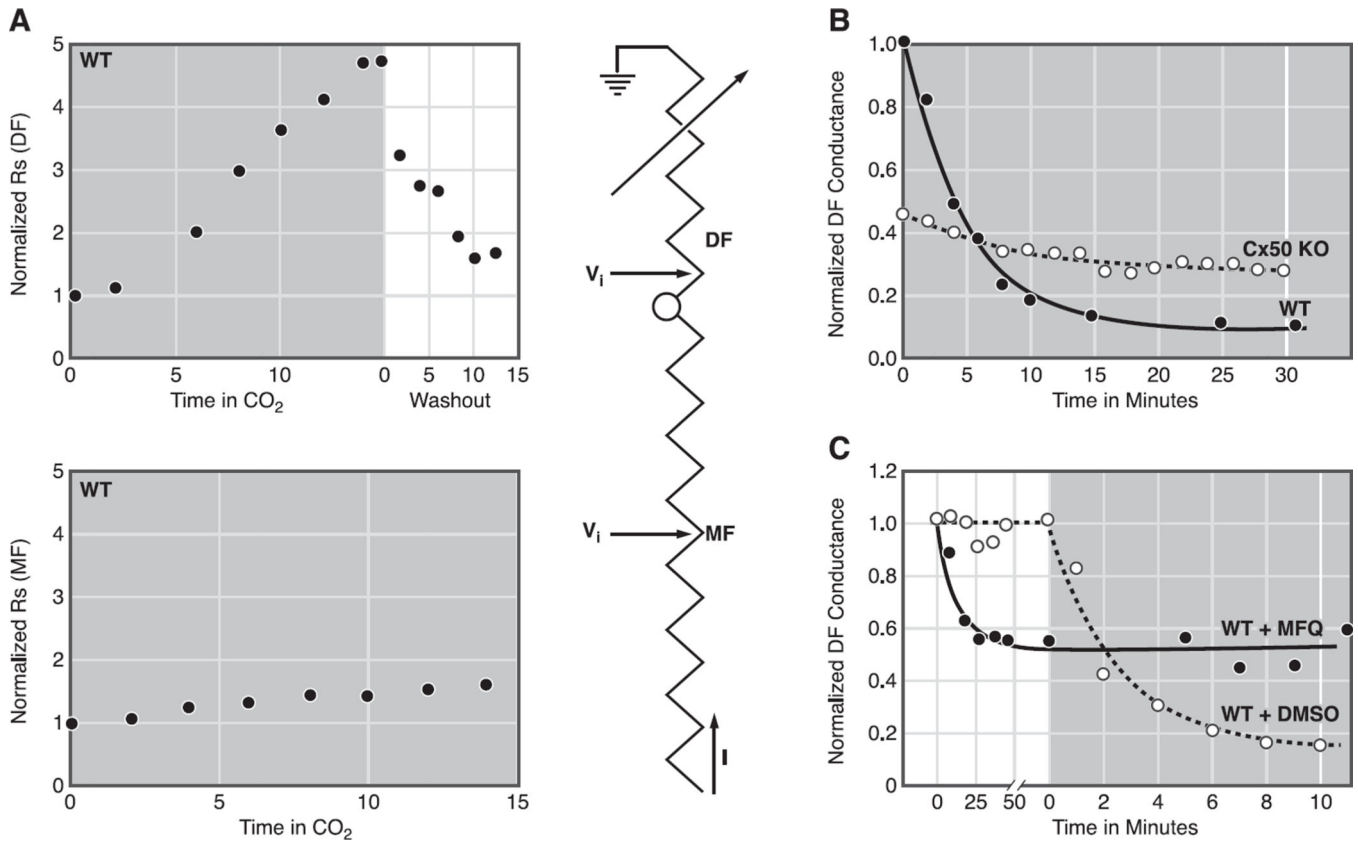
The methodology of whole lens impedance studies. *A*: the positioning of microelectrodes within the lens to inject current ( $I$ ) and measure the induced voltage ( $V$ ). The voltage microelectrode is moved to different locations to determine the spatial distribution of transport properties such as gap junction coupling conductance. *B*: typical records of the input impedance ( $R_{in}$ ) as a function of the sinusoidal frequency of the injected current. The data were recorded at four depths into the lens, starting at 12% of the distance into the lens from the surface ( $r/a = 0.88$ ), and culminating at 45% of the distance into the lens from the surface, where  $a$  is the radius and  $r$  is the distance from the center of the lens. Note the high frequencies, the input impedance asymptotes to a frequency-independent series resistance,  $R_S$ . As described in the text,  $R_S$  is proportional to the resistance of all the gap junctions between the point of voltage recording and the lens surface.

**Fig. 7.**

A summary of the properties of gap junction coupling in DF. **A:** the effects of knockout of Cx46 or Cx50 on coupling conductance of DF. The conductance has been normalized to the average value of wild-type (WT) coupling in DF, which is typically  $\sim 1 \text{ S/cm}^2$  of cell-to-cell contact, so the normalized values are close to actual values in those units. The reductions in conductance in Cx46<sup>+/-</sup> and Cx46<sup>-/-</sup> lenses are from Gong et al. (78). The reductions in conductance in Cx50<sup>+/-</sup> and Cx50<sup>-/-</sup> lenses are from Baldo et al. (8). The conclusion is that both Cx46 and Cx50 contribute to coupling of DF, and their contribution to the coupling conductance is about equal. **B:** immunostaining of connexins. The green labeling in *a* is for the inner loop of Cx46. The red labeling in *b* is for the COOH terminus of Cx50. The yellow labeling in *c* is an overlay of the two top panels and indicates both connexins are in the same plaques. The inner loop of Cx46 is not cleaved at the DF to MF transition, whereas the COOH terminus of Cx50 is cleaved, hence the green labeling persists into MF in *d*, whereas red staining does not. [From Gong et al. (78), copyright 1998 National Academy of Sciences USA.]

**Fig. 8.**

A summary of the properties of gap junction coupling conductance in the mature fibers (MF). *A*: the effects of knockout of Cx46 and Cx50 on MF coupling conductance. The conductances are normalized to the average value in the DF, which is  $\sim 1$  S/cm<sup>2</sup> of cell-to-cell contact. The reductions in coupling conductance in the Cx46<sup>+/-</sup> and Cx46<sup>-/-</sup> lenses are from Gong et al. (78). The data from Cx50<sup>+/-</sup> lenses are from Baldo et al. (8). In the MF of WT lenses, the average coupling conductance is about half that of DF. Knocking out half of Cx46 (Cx46<sup>+/-</sup>) caused a 50% reduction in MF coupling conductance, whereas knocking out all of Cx46 (Cx46<sup>-/-</sup>) reduced coupling to zero. In contrast, knocking out half of Cx50 (Cx50<sup>+/-</sup>) had no effect on MF coupling. In the Cx50<sup>-/-</sup> lenses, coupling decreased, but so did all transport parameters, suggesting indirect effects. The Cx50<sup>+/-</sup> lenses were perfectly healthy, but there was no effect on coupling, suggesting Cx50 does not contribute to MF coupling, consistent with the results from the Cx46<sup>+/-</sup> and Cx46<sup>-/-</sup> lenses. *B*: the effects of knockout (KO) and knock in (KI) of Cx46 on MF coupling conductance. The KO data are from Gong et al. (78). The KI data are from Martinez-Wittinghan et al. (127). The normalized MF coupling conductance is almost linearly proportional to the number of copies of Cx46 being expressed, suggesting Cx46 is the only functional connexin in the MF.

**Fig. 9.**

Gating of lens gap junction channels. **A:** gating of gap junctions in WT lenses. When current is injected into a central fiber cell and voltage recorded in DF, the series resistance ( $R_s$  in Fig. 6B) increases dramatically and reversibly when the lens is superfused with  $\text{CO}_2$  solution, indicating closure of DF gap junction channels. In contrast, when voltage is recorded in MF, the increase in series resistance is relatively small, indicating MF channels are not closing and the small increase is due to closure of DF channels. [From Martinez-Wittingham et al. (127), with permission from the Association for Research in Vision and Ophthalmology.] **B:** gating of DF gap junction channels in WT and Cx50 $^{-/-}$  lenses. KO of Cx50 reduces DF coupling conductance to about half its normal value, but the remaining Cx46 channels have lost most of their pH sensitivity. Because the KO lenses were in such poor condition, we thought the lack of gating might be an indirect effect, but this was ruled out by the data in **C**. [Redrawn from Baldo et al. (8).] **C:** gating of DF gap junction channels in WT and mefloquine-treated lenses. Mefloquine (MFQ) blocks gap junction coupling conductance in channels made from Cx50 but not Cx46. DF gap junction coupling conductance drops to about half its normal value over a period of  $\sim 1$  h in MFQ, suggesting blockade of all Cx50 channels, leaving Cx46 channels to provide coupling. When the MFQ lenses are superfused with  $\text{CO}_2$ -containing solution, there is no closure of the remaining Cx46 channels, whereas in the untreated lens, both Cx50 and Cx50 channels close. The MFQ-treated lens was perfectly healthy, so the small residual gating seen in Cx50 $^{-/-}$  lenses is actually due to their poor health, and in a healthy lens Cx46 channels are totally

insensitive to pH. [From Martinez-Wittingham et al. (128), with permission from Springer Science + Business Media.]

Author Manuscript

Author Manuscript

Author Manuscript

Author Manuscript



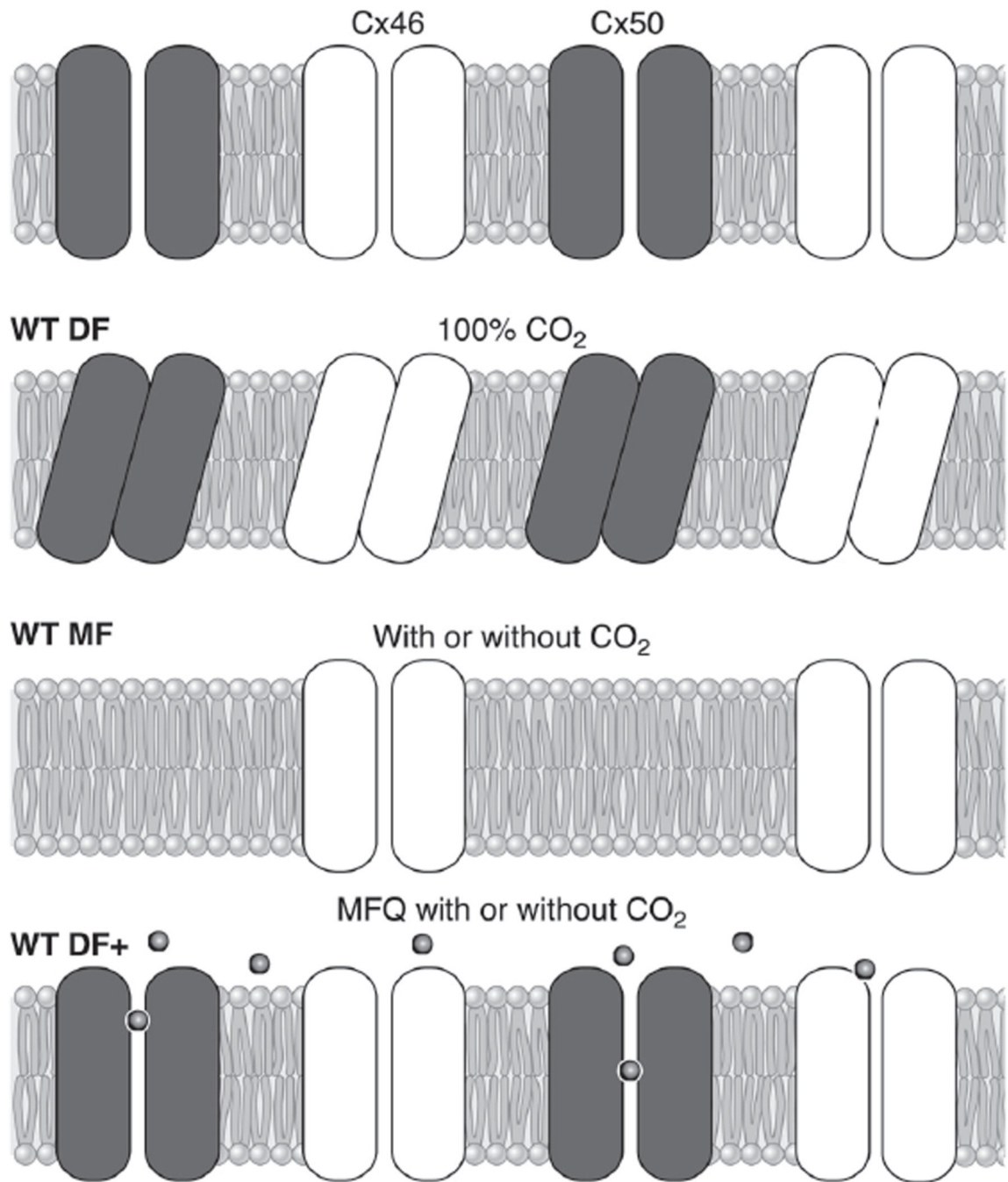
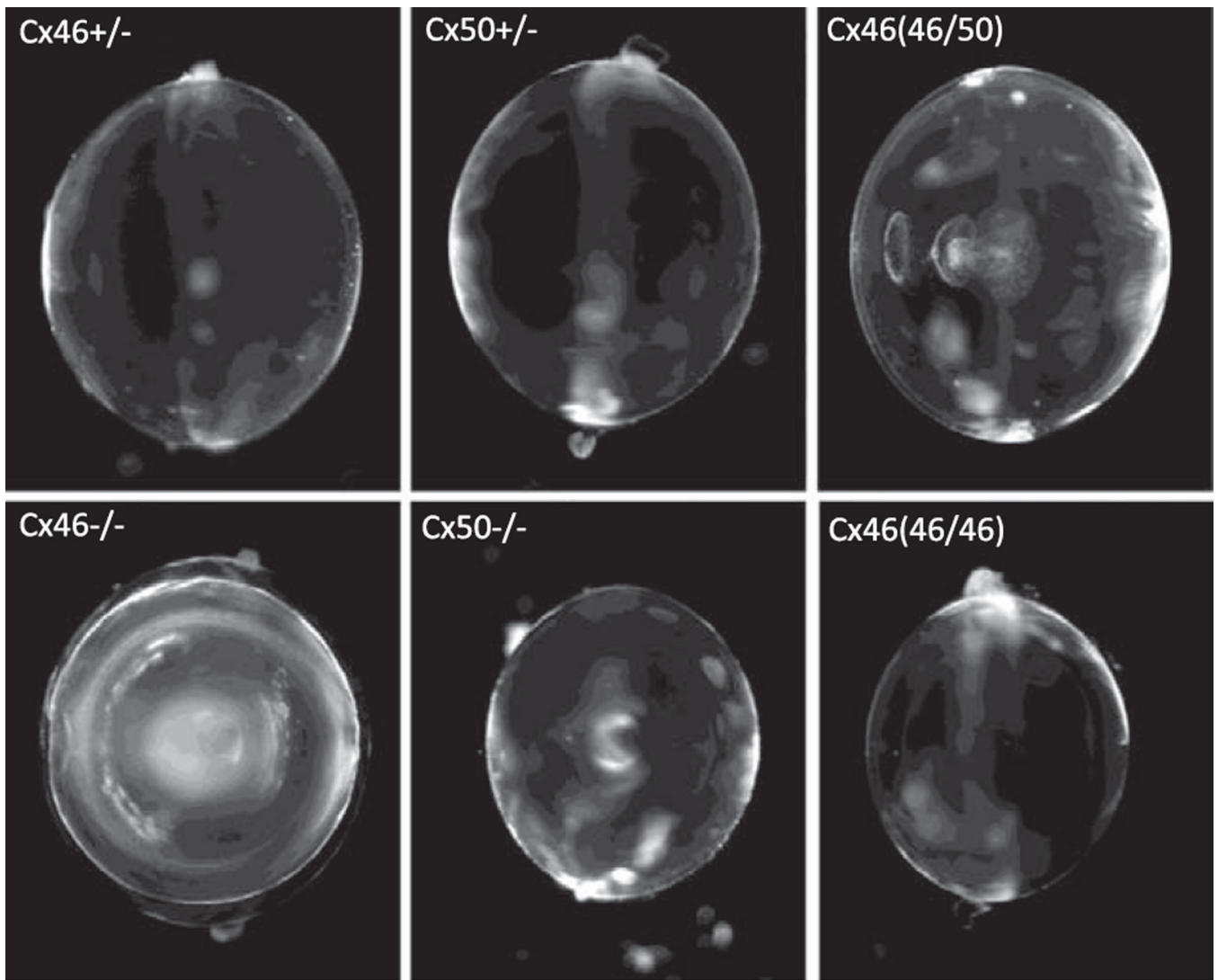


**Fig. 10.** A mode of cooperative gating to explain the data shown in Figure 9. [From Martinez-Wittingham et al. (128), with permission from Springer Science + Business Media.]



(photographed on their equatorial edge)

**Fig. 11.**

The effects of KO or KI of lens connexins on transparency. The Cx46+/- or Cx50+/- lenses are indistinguishable from WT, so a WT lens is not shown. Surprisingly, the Cx50(46/50) heterozygous KI lens gets a significant central cataract, even though its coupling conductance is at least as great as that of the Cx46+/- or Cx50+/- lenses. The Cx46-/- lens gets a dense central cataract. The Cx50-/- lens has a mild central cataract but is undersized and in poor physical shape. The Cx50(46/46) lens is as transparent as WT lenses, but it is undersized. It appears Cx50 is necessary for normal growth.

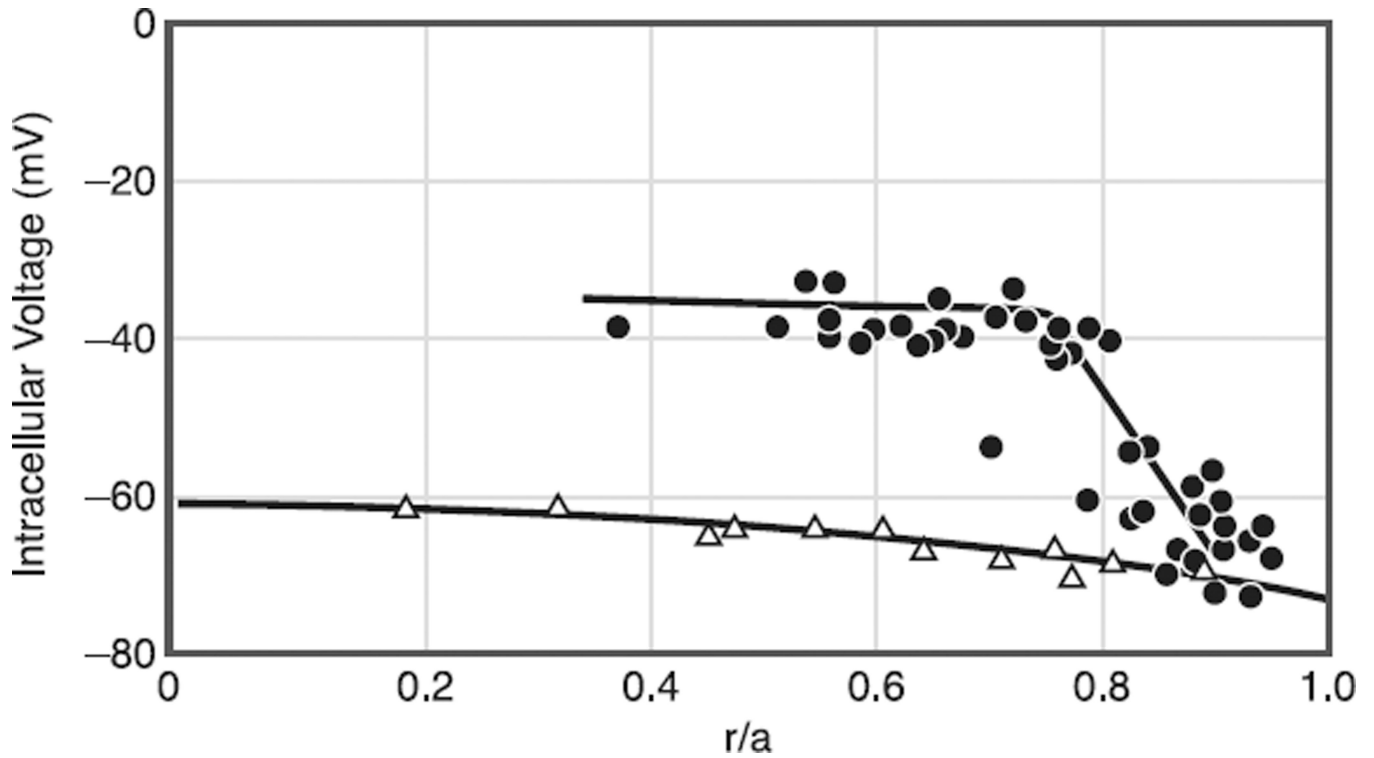


**Fig. 12.**

The radial variation in resting voltage in WT and Cx46<sup>-/-</sup> lenses. In WT lenses, there is about a 10-mV gradient between the central and surface fiber cells, as the voltage is about -60 mV in the center and drops to -70 mV at the surface. This is associated with the circulating ionic currents described in Figure 4. In the Cx46<sup>-/-</sup> lens, MF coupling is lost so the current cannot circulate through the MF and the voltage becomes flat. However, because the MF are also isolated from the epithelial K<sup>+</sup> channels, the cells depolarize to voltage dependent on their Cl<sup>-</sup> and Na<sup>+</sup> conductances. [From Gong et al. (78), copyright 1998 National Academy of Sciences USA.]

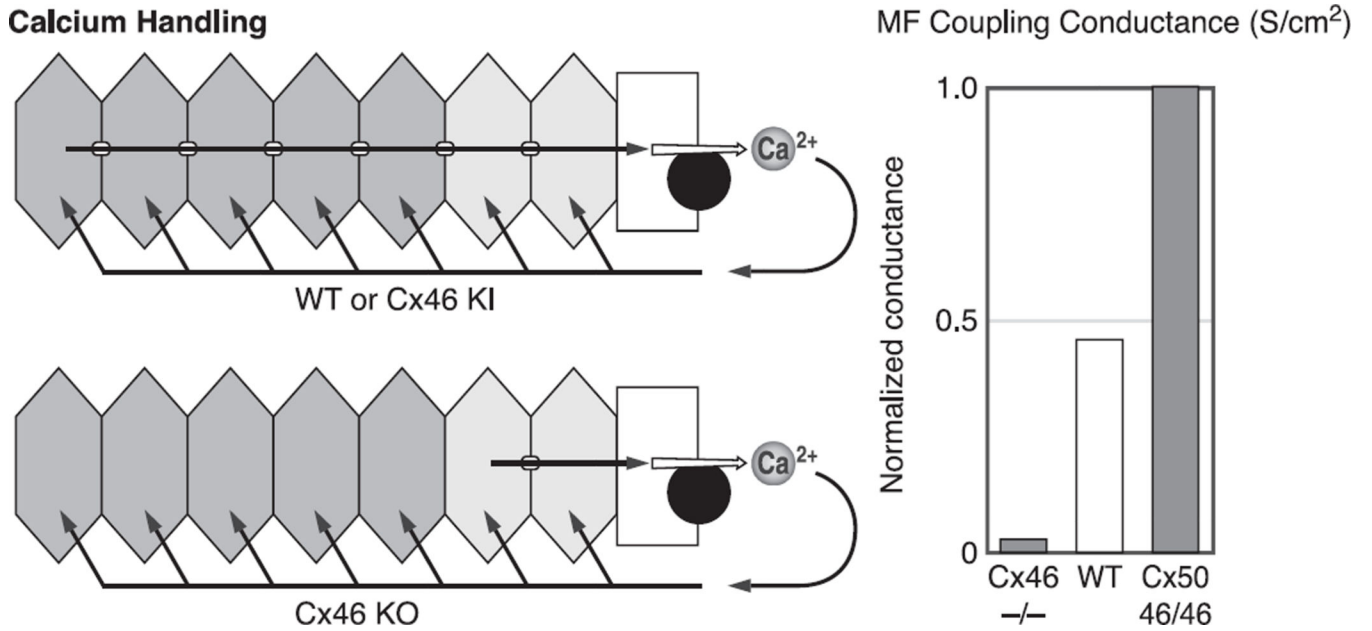


**Fig. 13.** Calcium homeostasis in the lens and its relationship to gap junction coupling conductance.  $Ca^{2+}$  is expected to circulate between the surface epithelial cells where active transport takes place and the inner fiber cells where the passive leak takes place. Thus a center-to-surface concentration gradient should exist to drive diffusion, and that gradient should depend on fiber cell coupling conductance. [From Gao et al. (66), copyright 2004. Originally published in *The Journal of General Physiology*.]

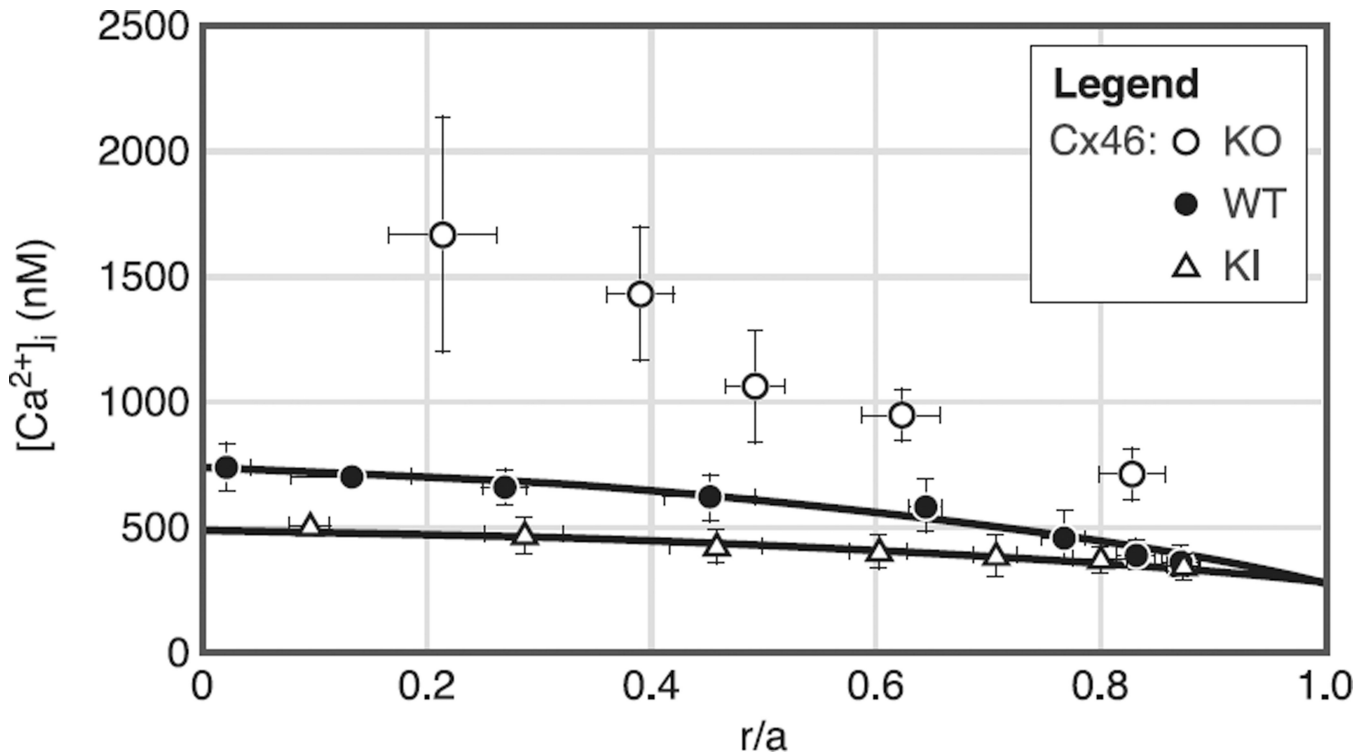


**Fig. 14.**

Calcium concentration gradients measured with fura 2 in intact lenses from WT and Cx46 KO and KI lenses. In WT lenses, there is a center-to-surface  $\text{Ca}^{2+}$  gradient of  $\sim 400$  nM, as the concentration goes from 700 nM at the center to 300 nM at the surface. In the Cx50(46/46) KI lenses, the MF coupling conductance is doubled and the concentration gradient is halved, now being 200 nM, as the concentration goes from 500 nM at the center to 300 nM at the surface. In the Cx46<sup>-/-</sup> KO lenses, the lack of MF coupling blocks the egress pathway for  $\text{Ca}^{2+}$ , so it accumulates without regulation in the MF. [From Gao et al. (66), copyright 2004. Originally published in *The Journal of General Physiology*.]

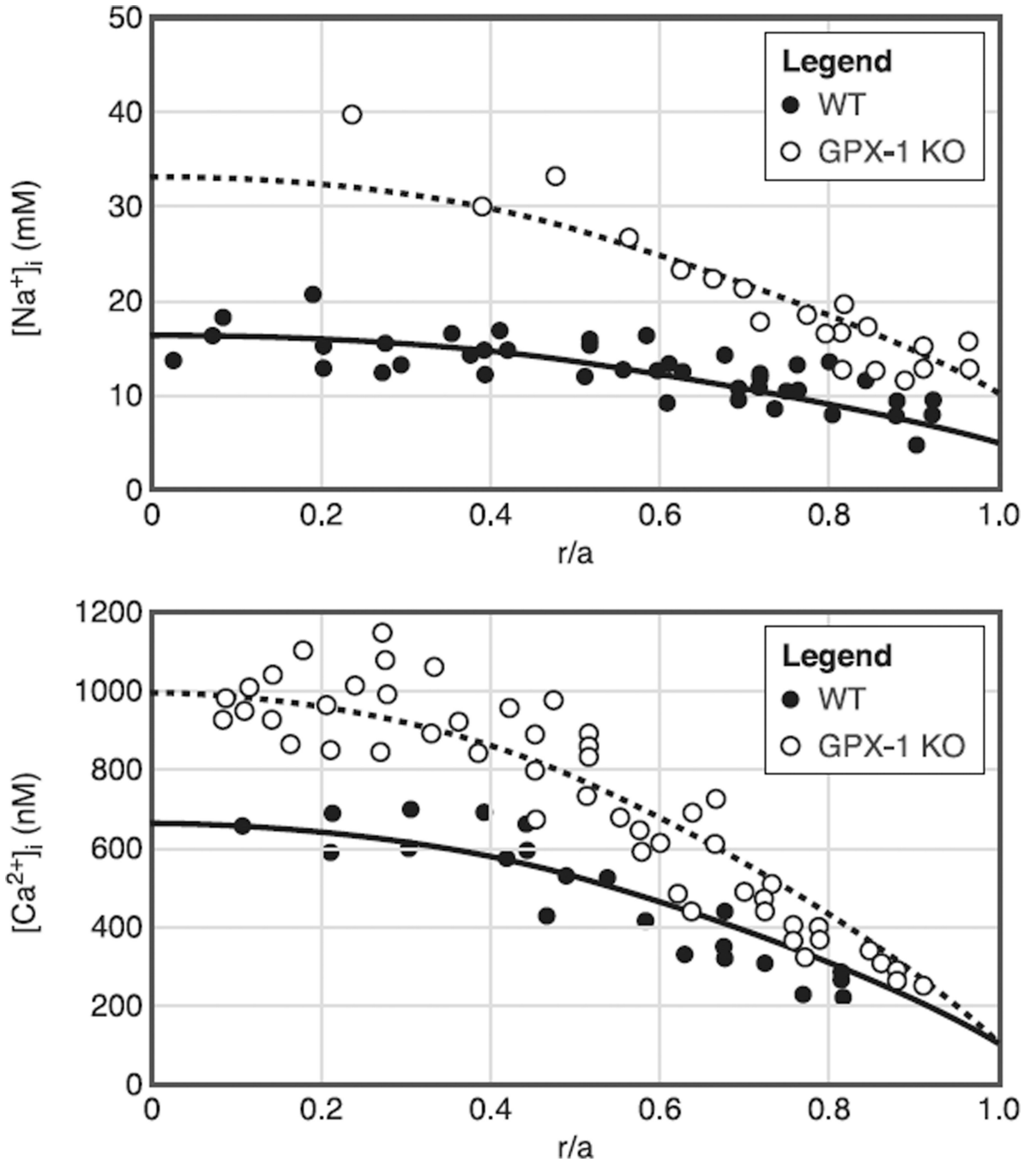


**Fig. 15.**

The effect on intracellular homeostasis of knocking out GPX-1, an enzyme that protects the lens against  $H_2O_2$ -mediated oxidative damage. All lenses were ~2 mo old. The smooth curves are from a structurally based model of the lens circulation. The only detectable defect in the GPX-1 KO lenses was that MF coupling conductance was on average half the value in WT lenses, so the expected effect is that the same circulation of  $Na^+$  or  $Ca^{2+}$  will require twice the center-to-surface concentration gradient. A: intracellular  $Na^+$  concentration gradients measured with SBF1 in WT and GPX-1 KO lenses. In WT lenses, the  $Na^+$



concentration gradient is ~10 mM, as the concentration goes from 17 mM at the center to 7 mM at the surface. In the GPX-1 KO lenses, the gradient is ~22 mM, as the concentration goes from 33 mM at the center to 11 mM at the surface. *B*: intracellular  $\text{Ca}^{2+}$  concentration gradients measured with fura 2 in WT and GPX-1 KO lenses. In the WT lens, the gradient is ~500 nM, as the concentration goes from 650 nM in the center to 150 nM at the surface. In the GPX-1 KO lenses, the gradient is ~850 nM, as the concentration goes from ~1,000 nM at the center to 150 nM at the surface. [From Wang et al. (204), with permission from Springer Science + Business Media.]

Author Manuscript

Author Manuscript

Author Manuscript

Author Manuscript

TABLE 1

## Connexin mutations in humans

Gene/Mutated Residue/Domain	Phenotypes
Cx50/R23T/NH <sub>2</sub> terminal	Dominant/progressive congenital nuclear cataract (220)
Cx50/V44E/E1 loop	Whole cataract with variable myopia microcornea (50)
Cx50/W45S/E1 loop	Bilateral cataract (201)
Cx50/D47N/E1 loop	Dominant nuclear pulverulent opacity, altered trafficking, a loss of function (7)
Cx50/D48K/E1 loop	Dominant nuclear pulverulent opacity (20)
Cx50/G64V/E1 loop	Dominant nuclear cataract (238)
Cx50/V79L/TM2	“Full moon” with Y-suture opacity (199)
Cx50/P88S/TM3	Zonular pulverulent cataract (182)
Cx50/P88Q/TM3	Lamellar pulverulent (7) or balloonlike cataracts (200)
Cx50/P189L/E2 loop	Star-shaped nuclear opacity with a whitish core (88)
Cx50/R198Q/COOH terminal	Posterior subcapsular cataract with variable myopia and microcornea (50)
Cx50/I274M/COOH terminal	Zonular pulverulent cataract (162)
Cx50/S276F/COOH terminal	Pulverulent nuclear cataract (227)
Cx50/255 frameshift/COOH terminal	Recessive triangular cataract (175)
Cx50/203 frameshift/COOH terminal	Recessive cataract (163)
Cx46/D3Y/NH <sub>2</sub> terminal	Dominant zonular pulverulent cataract (1)
Cx46/L11S/NH <sub>2</sub> terminal	Ant-eggs cataract (88)
Cx46/V28M/TM1	Varied cataracts (49)
Cx46/F32L/TM1	Dominant nuclear pulverulent opacity (97)
Cx46/R33M/TM1	Finely granular embryonic cataract (85)
Cx46/W45S/E1 loop	Progress nuclear cataract (123)
Cx46/P59L/E1 loop	Dominant nuclear punctuate cataract (19)
Cx46/N63S/E1 loop	Dominant cataract (124)

Cx, connexin. Reference numbers are given in parentheses.

**TABLE 2**

## Connexin mutations in rodents

<b>Gene/Mutated Residue/Domain</b>	<b>Phenotypes</b>
Mouse Cx50/G22R/NH <sub>2</sub> terminal	Dominant and ruptured lens (35)
Mouse Cx50/D47A/E1 loop	Dominant nuclear cataract No2 (187)
Mouse Cx50/S50P/E1 loop	Dominant cataract and microphthalmia (224)
Mouse Cx50/V64A/E1 loop	Dominant cataract (81)
Mouse Cx50/null (knockout)	Recessive nuclear cataract and microphthalmia
Mouse Cx46/null (knockout)	Recessive nuclear cataract
Rat Cx50/L7Q/NH <sub>2</sub> terminal	Semi-dominant and microphthalmia (119)
Rat Cx50/R340W	Semi-dominant cataract (226)
Rat Cx46/E42K/E1 loop	Recessive nuclear cataract (231)

Cx, connexin. Reference numbers are given in parentheses.